

REPORT DOCUMENTATION PAGE

*Form Approved
OMB No. 0704-0188*

The public reporting burden for this collection of information is estimated to average 1 hour per response, including the time for reviewing instructions, searching existing data sources, gathering and maintaining the data needed, and completing and reviewing the collection of information. Send comments regarding this burden estimate or any other aspect of this collection of information, including suggestions for reducing the burden, to Department of Defense, Washington Headquarters Services, Directorate for Information Operations and Reports (0704-0188), 1215 Jefferson Davis Highway, Suite 1204, Arlington, VA 22202-4302. Respondents should be aware that notwithstanding any other provision of law, no person shall be subject to any penalty for failing to comply with a collection of information if it does not display a currently valid OMB control number.

PLEASE DO NOT RETURN YOUR FORM TO THE ABOVE ADDRESS.

1. REPORT DATE (DD-MM-YYYY) 31-08-2005		2. REPORT TYPE Final		3. DATES COVERED (From - To) 13-09-2004 to 31-08-2005	
4. TITLE AND SUBTITLE Energy Finite Energy Analysis (EFEA) Algorithms & Software for Ship Noise				5a. CONTRACT NUMBER N00014-04-C-0448	
				5b. GRANT NUMBER	
				5c. PROGRAM ELEMENT NUMBER	
6. AUTHOR(S) Gilroy, Layton; Brennan, David; Boroditsky, Leo; Fischer, Ray; Koko T.S; Akpan, U.O; Dunbar, T.E; and Seto, Mae				5d. PROJECT NUMBER	
				5e. TASK NUMBER	
				5f. WORK UNIT NUMBER	
7. PERFORMING ORGANIZATION NAME(S) AND ADDRESS(ES) Noise Control Engineering, Inc. 799 Middlesex Turnpike Billerica MA 01821				8. PERFORMING ORGANIZATION REPORT NUMBER NCE TM 05-029	
9. SPONSORING/MONITORING AGENCY NAME(S) AND ADDRESS(ES) Office of Naval Research, ONR Ballston Tower One 800 North Quincy St. Arlington VA 22217-5660				10. SPONSOR/MONITOR'S ACRONYM(S) ONR	
				11. SPONSOR/MONITOR'S REPORT NUMBER(S)	
12. DISTRIBUTION/AVAILABILITY STATEMENT Unclassified/Unlimited DISTRIBUTION STATEMENT A Approved for Public Release Distribution Unlimited					
13. SUPPLEMENTARY NOTES Prepared in cooperation with Defence Research and Development Canada (DRDC) and Martec, Inc.					
14. ABSTRACT This Phase I report explores the feasibility of using Energy Finite Element Analysis (EFEA) methods for structural acoustic applications. Using both Statistical Energy Analysis (SEA) and experimental results as benchmarks, the steady-state power flow capabilities EFEA software are demonstrated. Results obtained via the power flow finite element approach are generally in good agreement with those obtained elsewhere. Development and implementation of capabilities for predicting reverberant interior and underwater-radiated noise (including machinery- and flow-related) are also discussed. A number of recommendations are outlined concerning further improvements to the EFEA software that would enhance its attractiveness as a provisional tool for EFEA. The ideal implementation would be a hybrid system of EFEA and SEA for the analysis and understanding of ship noise and vibration. The EFEA approach would be appropriate for structureborne energy flow in and around the source, where the vibration gradient is high, and the SEA approach would be appropriate for modeling the transport of energy away from the machinery space.					
15. SUBJECT TERMS noise prediction, Energy Finite Element Analysis (EFEA), Statistical Energy Analysis (SEA), hydroacoustic analysis, ship noise, underwater radiated noise					
16. SECURITY CLASSIFICATION OF:			17. LIMITATION OF ABSTRACT UU	18. NUMBER OF PAGES 62	19a. NAME OF RESPONSIBLE PERSON Raymond W. Fischer
a. REPORT U	b. ABSTRACT U	c. THIS PAGE U			19b. TELEPHONE NUMBER (Include area code) 978-670-5339

TECHNICAL MEMO 2005-029



***Energy Finite Element Analysis (EFEA) Algorithms and
Software for Ship Noise (Phase 1)***

Layton Gilroy (DRDC)
David Brennan (Martec)
Leo Boroditsky (NCE)
Ray Fischer (NCE)
T.S. Koko (Martec)
U.O. Akpan (Martec)
T.E. Dunbar (Martec)
Mae Seto (DRDC)

August 31, 2005

Contract No. N00014-04-C-0448
NCE JOB No. J04-047

Prepared for:
Mr. Steven Schreppler
ONR US Navy

DISTRIBUTION STATEMENT A
Approved for Public Release
Distribution Unlimited

Prepared by:
NOISE CONTROL ENGINEERING, Inc.
799 Middlesex Turnpike
Billerica, MA 01821
978-670-5339
978-667-7047 (fax)
nonoise@noise-control.com
<http://www.noise-control.com>

20050907 036

TABLE OF CONTENTS

ABSTRACT	1
1. INTRODUCTION	1
2. OVERVIEW OF PFFEAS RESEARCH STUDIES	2
3.0 OVERVIEW OF SNAP SOFTWARE	6
3.1 Pre-Processing (PFGEN).....	6
3.1.1 Heat Conduction Solver (VASTF).....	7
3.1.2 Post-Processing (PFPOST).....	7
3.1.3 Creating SNAP Models.....	7
3.2 Theoretical Foundations.....	7
3.2.1 Power Flow Equations for Beams and Plates.....	7
3.2.2 Treatment of Junctions.....	12
3.2.3 Fluid Modelling.....	16
4. VALIDATION OF SNAP	18
4.1 Simple Beam (Flexural Loading).....	18
4.2 Cantilever Beam (Axial Loading).....	21
4.3 Two Coupled Beams With Boundary Conditions.....	24
4.4 General Square Plate.....	25
4.5 Rectangular Plate.....	28
4.6 Two Rectangular Beams at Right Angles (Flexural Load).....	30
4.7 Two Rectangular Beams at Right Angles (Axial Load).....	31
4.8 Two Rectangular Plates at Right Angles (Flexural Load).....	32
4.9 Stiffened Box Structure.....	34
5. TRANSIENT ENERGY FINITE ELEMENT ANALYSIS CAPABILITY	41
5.1 Review of Transient SEA Analysis and Presentation of Transient EFEA Requirements.....	41
6. HABITABILITY AND UNDERWATER RADIATED NOISE	43
6.1 Interior Noise.....	43
6.2 Radiated Noise.....	44
6.2.1 Reverberant Panel.....	46
6.2.2 Panel with Applied Load.....	46
6.2.3 Energy Fields.....	47
6.3 Experimental Results.....	48
7. FLOW-INDUCED NOISE	48
7.1 Modeling Flow-Induced Noise within EFEA.....	49
7.2 Recommendations for Implementation.....	50
8. EFEA SUMMARY	52
9. SEA AND EFEA ENERGY METHODS FOR NOISE PREDICTION AND CONTROL	53
10. EFEA IMPLEMENTATION IN PRACTICE	56
11. REFERENCES	58

ABSTRACT

This Phase I report explores the feasibility of using Energy Finite Element Analysis (EFEA) methods for structural acoustic applications. Power Flow Finite Element Analysis (PFFEA) methodology is reviewed to assess its potential for use in investigating structural acoustic modeling throughout the medium- and high-frequency regimes. Past EFEA/PFFEA research is reviewed, along with a discussion surrounding the development and implementation of EFEA/PFFEA methodologies into the 'SNAP' software package developed by DRDC. Application of the power flow approach to structural elements such as nodes, beams, connections, and membranes is also presented, along with a review of power flow strategies for fluid-loaded structures. Using both Statistical Energy Analysis (SEA) and experimental results as benchmarks, the steady-state power flow capabilities of the SNAP software are demonstrated using both simple beam models and more complex structural models. Results obtained via the power flow finite element approach are generally in good agreement with those obtained elsewhere, suggesting that the EFEA/PFFEA methodology currently featured in the SNAP software could greatly compliment existing SEA techniques, and may prove an effective tool for response prediction in the medium- to high-frequency domain. By enhancing existing SNAP capabilities, it is envisioned that the software could be presented as a provisional tool for EFEA. A review of transient energy methods suggests that its implementation for EFEA is indeed feasible. A number of practical issues concerning the implementation of transient EFEA are also identified. Development and implementation of capabilities for predicting reverberant interior and underwater-radiated noise (including machinery- and flow-related) are also discussed. A number of recommendations are outlined concerning further improvements to the SNAP software that would enhance its attractiveness as a provisional tool for EFEA.

At this point the authors feel the ideal implementation would be a hybrid system of EFEA and SEA for the analysis and understanding of ship noise and vibration. The EFEA approach would be appropriate for accounting for structureborne energy flow in and around the source, where the vibration gradient is high, and the SEA approach would be appropriate for modeling the transport of energy away from the machinery space.

Sections 1 through 8 were prepared by Martec and DRDC Atlantic. Sections 9 and 10 were developed by Noise Control Engineering, Inc

1. INTRODUCTION

Ship structural characteristics such as acoustic signature, flow noise, internal airborne noise, and vibration response to transients or shock are difficult to model efficiently and accurately with existing tools. Methodologies such as Power Flow Energy Finite Element Analysis (PFEFEA) may offer a potential alternative to circumvent these difficulties during ship structural design. The feasibility of advancing PFEFEA into the mainstream of naval ship design must first be researched and compared to other predictive tools such as Statistical Energy Analysis (SEA). The current study is focused on issues relating to structural acoustic modeling for EFEA purposes. This report

constitutes the first of a possible three-phase study into the potential for PFEFEA application, and centers on the assessment and state-of-the-art of this methodology.

Power flow energy finite element analysis (PFEFEA) is a relatively new technology used to investigate structural response throughout the high-frequency regime where traditional Finite Element Analysis (FEA) may be impractical. Traditional finite element programs are not well suited for use in the high-frequency regime because a very detailed mesh is often needed to accurately capture the modal deformation of the structure, which may be prohibitively expensive in terms of the array size and computational time required. To overcome these limitations, acousticians commonly rely on statistical energy analysis (SEA) techniques. The SEA approach uses averaging assumptions with regards to the energy within each subsystem (i.e., members between joints), thereby producing discrete results for each subsystem. The PFEFEA approach may be a good compliment or alternative to using SEA, as it predicts a spatially- continuous variation of vibrational energy over the entire structure, thereby allowing point- response predictions within a subsystem. Martec Limited and DRDC Atlantic (Defense Research and Development Canada, formerly Defense Research Establishment Atlantic (DREA)) have been investigating the power flow regime for over a decade [1-10]. Much of the knowledge gained over this period, from both numerical and experimental research has been incorporated into a suite of programs entitled "SNAP". The SNAP software has been developed to automate the power flow process, allowing the user to perform a high-frequency analysis with little knowledge of the internal power flow calculations. The main focus of this report is to examine the existing SNAP software capabilities, assess its potential for noise prediction, highlight its limitations, provide recommendations for further improvement of its capabilities, and adapt the software to accommodate modeling high-frequency transient/shock problems.

Section 2 provides highlights of the power flow energy finite element analysis developmental work performed by DRDC Atlantic and Martec Limited over the past decade. A summary of the state of the SNAP software and its theoretical foundations are presented in Section 3. Validation of the SNAP software, including a description of the test cases used, is discussed in Section 4. Section 5 investigates the feasibility of implementing transient energy flow methodologies and capabilities. Habitability and radiated noise are presented in Section 6, while flow noise is reviewed in Section 7. Conclusions and recommendations for enhancing the modeling and analysis capabilities (to be executed during Phase II and III of the project) are then provided in Section 8. Section 9 assesses the EFEA approach versus SEA and Section 10 considers the implementation of EFEA in practice.

2. OVERVIEW of PFEFEA RESEARCH STUDIES

This section provides a summary of the PFEFEA development studies performed by Martec Limited and DRDC Atlantic from the period from 1989 to 1999. The first of these studies was performed by Burrell (1989). This study laid the groundwork for future investigations of the PFEFEA method and demonstrated its applicability for the analysis of structural and acoustic systems at high frequencies. Burrell identified PFEFEA as a tool

intended for the analysis of structural and acoustic systems at high frequencies where the standard finite element method is not practical due to the large number of elements required to accurately capture the modal deformations. Like SEA, PFFEA was developed using the conservation of vibration energy concept. However, PFFEA predicts smooth approximations and is spatially continuous within a structural component, while SEA is a single average for a subsystem. This is the first indication that PFFEA may be an ideal tool for modeling areas in the immediate vicinity of any equipment where foundations, framing and plating vary significantly. Furthermore it was shown that PFFEA could be solved using a thermal finite element analysis, and hence has the potential to be incorporated into existing finite element programs. PFFEA requires few elements (coarse mesh) for convergence and is considered more efficient than regular finite element analysis. Structures investigated by Burrell included a single beam, two coupled beams and a circular plate, using hand calculations and ANSYS finite element software. The main disadvantages of PFFEA was identified as its inability to predict an accurate response near points of loading and boundaries (Burrell, 1989)

Following the initial studies, a three-year study was undertaken in order to develop a PFFEA capability for DRDC Atlantic. In Year I, Burrell and Chernuka (1990) extended the theory to include rectangular plates. Although the theory was developed, implementation was not carried out. The main highlights of the study included the following:

- Bending, longitudinal, transverse, and torsional wave types were identified as relevant for PFFEA of structures of interest (beams and plates). (Designer Noise¹ – the SEA implementation specific to ships, only considers bending waves.)
- Different wave types can be incorporated into general PFFEA theory through appropriate values of group velocity (c) and input power. These are summarized in Section 3.
- Implementation of VASTF, a finite element software for heat transfer, was started
- Simultaneous propagation of waves was investigated and it was found that the different waves can be treated as independent for each member, but are coupled at junctions
- Lumped masses are best addressed at junctions
- A general PFFEA junction was developed, but junctions between beams and plates was not addressed

In the second phase of the study, Burrell et al (1992) extended the PFFEA modeling capabilities developed during Phase 1. This work revisited the fundamental assumptions of the PFFEA, further investigated the benefits of PFFEA and investigated the valid frequency ranges for PFFEA. Highlights of the study are provided below:

- It is necessary to model in-plane vibrations
- Input impedances for beam-plate combinations could be represented by the corresponding impedance for the beam alone
- Diffuse energy fields could be assumed (fundamental to modeling plate junctions)

¹ Designer Noise™ is the shipboard noise prediction software package produced by NCE and Proteus as a result of SBIR 98-092.

- Junction theory was investigated by examining kinetic energy density ratio method, the wave transmission approach, and the Receptance method.
- Wave transmission approach was considered the best, although kinetic energy density ratio method is occasionally used
- Plate junctions fully investigated, but the definition of transmission efficiencies not carried out
- Beam-plate junctions modeling was started
- VASTF linear analysis was implemented and recommendations for future implementation of transient and non-linear capabilities were provided.

In the third phase of the work, Burrell et al, (1992) performed numerical investigations of rectangular plates excited in flexure, beams excited longitudinally, beam-beam and plate-plate junctions, and started investigations of plate-beam junctions. The highlights of the investigations are provided below:

- Development of pre- and post-processor for VASTF started
- Beam-beam junctions were thoroughly investigated
- Modeling of mode conversions and simultaneous conduction of different modes are demonstrated for the first time
- Plate-plate junctions were presented although actual formulations were not derived
- Preliminary investigation of beam-plate junctions started. A simplified model was developed which assumes that stiffeners do not participate in the conduction of energy but rather act as blocking masses
- Modeling of ring stiffened cylinders and stiffened plates (with example) were considered

Smith and Chernuka (1996) continued the work of Burrell, modeling more complex structural configurations, such as stiffened plates and shells. They developed energy transmission models for three dimensional beam junctions modeled, with and without shear deformation and rotary inertia in the formulation. Methodologies for energy transmission of complex plate junctions and beam-plate junctions were also investigated and demonstrated. A preliminary investigation into the application of PFFE in fluid-structure interaction was also provided. Below is a summary of the observations and some of the conclusions reached from their study:

- Shear deformation may cause a substantial difference in transmission efficiencies of a junction even at frequencies below the range where shear mode propagation occurs, therefore the use of Timoshenko junction model at upper range for beams was recommended
- Offset connection points, due to size of connecting members, can be more significant than shear deformation
- A translator program called PFGEN was created to automatically generate the equivalent power flow heat transfer models for VASTF. Structural configurations that can be modelled include beams, plates, and plate-beam junction models (beam, bar, membrane, and plate elements).
- Deficiencies in the modeling of applied load input power were identified. Some of these include the need for a more extensive treatment of load types (i.e. line loads and in-plane excitation of plate); provisions for relative phasing of applied loads; ability

to differentiate between boundary loads and interior loads; and capability for boundary reflections in the input power.

- It was recommended that the translator should in the future support the application of lumped masses, external constraints, and discrete damping elements. Also, it was recommended that a post processor be developed to convert VASTF results to structural results in a user-friendly manner.
- From the example problems considered, discrepancies attributed to the assumption of infinite beams in the input power and junction calculations were discovered, and hence improvements in the input power options were suggested for future consideration as well as algorithms for junction transmissibility.
- When using large heavily damped plates it was observed that the driving point velocity is typically higher than PFEA predictions. This was attributed to differing characteristics of cylindrical-wave and diffuse field power flow (diffuse is not justified when cylindrical-wave dominates)

Smith and Chernuka (1996) performed experimental studies to validate the PFEA formulations for plate-beam systems. A Laser Doppler Vibrometer (LDV) and a force transducer were proposed to measure vibrational response and power flow in beam, plate-beam specimens, and a stiffened plate section of a real ship hull. Experiments were performed on three specimens; two of these specimens had layers of elastomeric damping material attached to suppress the reflection of flexural waves. The main objective of the study was to describe a measurement apparatus and procedure to determine power flow in a plate-beam system. It was shown that power flow could be measured on a beam using the LDV and a force transducer. Sinusoidal force testing produces were found to provide more reliable results than random noise testing. The test specimens were scaled down models of the actual structures and reflection of flexural waves was suppressed. The nature of power transmission, was poorly understood and recommendations for further investigations were provided.

Smith and Chernuka (1997) performed further investigations of the power flow method by developing more advanced capabilities. Formulas for structural input power and fluid modeling were developed. The total load and power flow for individual plates were derived in terms of Fourier transforms of velocities, forces and moments. Validation of T-shaped beams provided confirmation that the results were accurate in a frequency average sense. In addition, a new beam junction model was developed such that lumped mass and offset connection points were used to represent physical junction size. This new junction, along with thick-beam formulations, extended the frequency range over which numerical results were accurate. It was observed that beam-plate structures give accurate results for force-excitation of infinite stiffened and un-stiffened plates; however, difficulties were encountered in validating moment-excitations. More complex beam-plate configurations could not be validated for lack of suitable numerical / experimental results. A method for calculating the far field energy and intensity fields produced by a vibrating surface in a fluid was presented. However, it was recommended that more validation work was required.

Smith and Brennan (1998) further extended the PFFEAs capabilities and performed experimental validation of the methodology. Comparison between PFFEAs predictions and measured responses were provided for both a ring stiffened cylinder and a ship tank test structure. Furthermore, validation of a round robin stiffened panel was undertaken by comparing results generated by PFFEAs to predictions generated by the Direct Dynamic Stiffness Matrix Method (DDMM). Improvements to the pre-processor PFGEN were implemented to improve the input power models. Good correlations were obtained for T- and L-plate junctions. Results for a ship tank were better than results for a ring-stiffened cylinder, partially because the ship tank had better measurement procedures. The authors recommended that further measurements for beam plate junctions be carried out as well as the measurement of high frequency sound radiation from a submerged surface (which would be used to validate energy radiation model). In addition, the authors recommended that future work be performed to automate the element grouping and to implement the sound radiation capability. However, at the conclusion of this study, the authors stated that the SNAP program has all the features necessary for performing high frequency response analysis on most ship-like structures.

3.0 OVERVIEW of SNAP SOFTWARE

SNAP is a computer tool for analyzing the high frequency vibration response and noise transmission in ship structures. SNAP is based on the power flow finite element method (PFFEAs). The SNAP program has been designed to use structural finite element models (comprised of beam, plate and shell elements) as input. The SNAP system is comprised of three program modules: PFGEN, VASTF and POSTPF. A complete analysis requires the three programs to run in sequence. Each of these programs is a stand-alone executable that could be run separately or together under the SNAP driver program. General descriptions of the three programs are provided below. (SNAP User's Manual, 1998).

3.1 Pre-Processing (PFGEN)

This program reads the SNAP input files, reads the VASTF geometry and elements, and generates a PPFEM model. Three essential steps are required for generating a PPFEM model:

1. Finite elements must be converted to PPFEM elements using the conductivity modelling technique. This is done automatically in PFGEN. Existing structural elements in the FE model are replaced by elements of a similar type in the PPFEM model, but with different constitutive properties and degrees-of-freedom.
2. Structural junctions must be identified and junction conductivities calculated. Structural junctions are defined in the SNAP input file PREFIX.JNC. Junction conductivities provide the link through which energy can travel from one component to another. They are also responsible for converting, or scattering, one type of energy (e.g. flexural) into other types (e.g. longitudinal or shear).
3. Concentrated dynamic loads must be read and converted to source input power terms. Loads are defined in the SNAP input file PREFIX.LOD as steady-state load amplitudes at the frequency of interest.

3.1.1 Heat Conduction Solver (VASTF)

VASTF is a general-purpose program for FE analysis of thermal and other field-equation type problems. Detailed information on VASTF can be obtained from the VASTF Version 6.1 User's Manual (1996), but it is not necessary to refer to it to run SNAP. PFGEN sets up all the required VASTF input files for a SNAP analysis. VASTF computes the nodal energy levels and energy flux quantities in the system.

3.1.2 Post-Processing (PFPOST)

POSTF is an output translator for PFGEN and VASTF. VASTF output is in a form difficult to interpret, because VASTF node numbering is different from the node numbering in the original model, and because VASTF field variables are not of a form useful for engineering purposes. Both of these shortcomings are corrected by POSTF. The node numbers are restored to those of the original model, and the output variables are converted to any of six user-defined output types (displacement, velocity, acceleration, energy, intensity, and dissipated energy). Formatted output appears in a PREFIX.PFA file.

3.1.3 Creating SNAP Models

A SNAP model consists of:

- Geometry and elements (VAST format);
- Energy group definitions;
- Structural junction definitions;
- Dynamic loading data; and
- Lumped stiffness, mass and damping elements.

The first four of these are essential to every SNAP model.

The user must provide a master input file called PREFIX.USE. This is because all SNAP runs require essentially the same program steps.

The structure and format of the USE file is described in the following sections.

3.2 Theoretical Foundations

3.2.1 Power Flow Equations for Beams and Plates

The theoretical foundations on which the SNAP program is based have been developed in the research studies by Martec and DRDC Atlantic from 1989 to 1999 (a summary of this work is provided above in Section 2). The detailed derivations of the relevant equations can be found in the associated reports listed in the reference section, and as a result will not be repeated here. However, for the sake of completeness, a summary of some of the relevant expressions used to compute power flow is presented in this section.

The equations used by SNAP to represent power flow in beams and plates are based on formulations derived by Nefske and Sung (1989) and are provided below in Equations [3-1] and [3-2].

$$\bar{q} = -\lambda \nabla(l_c \mathbf{e}) \quad [3-1]$$

and

$$\frac{\partial \mathbf{e}}{\partial t} = \nabla \cdot \lambda \nabla(l_c \mathbf{e}) - \delta \mathbf{e} \quad [3-2]$$

where:

\bar{q} = power flux

\mathbf{e} = energy density

λ, l_c = PFFEA energy conduction parameters

δ = PFFEA energy dissipation parameter.

Nefske and Sung (1989) used these relationships to apply the PFFEA to a beam. As the expressions are independent of the coordinate system or number of degrees of freedom, they should be equally valid for plates, for example. Hence, applying the PFFEA to plates requires only the determination of λ, l_c and δ . Burrell (1989) stated that the dissipation parameter δ was actually the same for both a beam and a plate, and thus formulating the PFFEA system for a plate is further reduced to determination of the conduction parameters λ and l_c .

To determine λ and l_c for the beam, Nefske and Sung (1989) had conducted a wave propagation analysis in which an energy balance was performed on a control volume. A similar analysis was performed by Burrell et al. (1989, 1990, 1992a,b) on a plate structure. It can be shown that the energy conduction parameters have the following relation to the structural dynamic properties:

$$\lambda = \frac{c}{\omega \eta} \quad l_c = c \quad [3-3]$$

where c is the group velocity, ω the frequency of excitation and η the dynamic loss factor. In Table 3-1, the power flux relations for rods, beams, membranes, plates and their assumptions and restrictions are summarized.

Table 3-1: Power Flow Relationships and Restrictions

Structure	Power Flow Relationships	Assumptions & Restrictions
Rod	$\langle q \rangle = -\frac{c^2}{\eta\omega} \frac{d}{dx} \langle e \rangle$ $\frac{d^2 \langle e \rangle}{dx^2} - \left(\frac{\eta\omega}{c} \right)^2 \langle e \rangle = 0$	Time Averaged Light Damping
Beam	$\langle \bar{q} \rangle_{ff} = -\frac{c^2}{\eta\omega} \frac{d}{dx} \langle \bar{e} \rangle_{ff}$ $\frac{d^2 \langle \bar{e} \rangle_{ff}}{dx^2} - \left(\frac{\eta\omega}{c} \right)^2 \langle \bar{e} \rangle_{ff} = 0$	Time Averaged space Averaged Light Damping Farfield Only
Membrane	$\langle \bar{q} \rangle = -\frac{c^2}{\eta\omega} \nabla \langle \bar{e} \rangle$ $\nabla^2 \langle \bar{e} \rangle - \left(\frac{\eta\omega}{c} \right)^2 \langle \bar{e} \rangle = 0$	Time Averaged Space Averaged Light Damping
Plate	$\langle \bar{q} \rangle_{ff} = -\frac{c^2}{\eta\omega} \nabla \langle \bar{e} \rangle_{ff}$ $\nabla^2 \langle \bar{e} \rangle_{ff} - \left(\frac{\eta\omega}{c} \right)^2 \langle \bar{e} \rangle_{ff} = 0$	Time Averaged Space Averaged Light Damping Farfield Only

In this table, e is the energy density, the $\langle \rangle$ indicates time-averaged, a bar over a parameter indicates space-averaged, the subscript ff denotes far field, and arrow over q indicates that power flow becomes a vector quantity for the membrane and plate. The group velocities, c , and are different for each structure, and are summarized in Table 3-2. Power flow expressions for the various structure types are provided in Table 3-3.

Table 3-2: Summary of Group Velocities

Wave	Structure	Beam	Plate
Quasi-Longitudinal		$c = \sqrt{\frac{E}{\rho}}$	$c = \sqrt{\frac{E}{\rho(1-\nu^2)}}$
Torsional		$c = \sqrt{\frac{GQ}{J}}$	
Transverse			$c = \sqrt{\frac{E}{\rho}}$
Bending (Thin)*		$c = 2 \left[4 \frac{EI}{\rho A} \right] \sqrt{\omega}$	$c = 2 \left[4 \frac{EI'}{\rho h (1-\nu^2)} \right] \sqrt{\omega}$
Bending (Thick)		$c = \frac{2V^3}{\left[2V^2 - \omega \frac{d(V^2)}{d\omega} \right]}$ $V^2 \text{ and } \frac{d(V^2)}{d\omega} \text{ are given below, where:}$ $\alpha^2 = \sqrt{\frac{EI}{\rho A}}$ $\beta = \frac{I}{A} \left[1 + \frac{E}{Gl_c^2} \right]$ $\gamma = \frac{\rho l}{AGl_c^2}$	$c = \frac{2V^3}{\left[2V^2 - \omega \frac{d(V^2)}{d\omega} \right]}$ $V^2 \text{ and } \frac{d(V^2)}{d\omega} \text{ are given below,}$ where: $\alpha^2 = \sqrt{\frac{EI'}{\rho h (1-\nu^2)}}$ $\beta = \frac{I'}{h} \left[1 + \frac{E}{(1-\nu^2)Gl_c^2} \right]$ $\gamma = \frac{\rho l'}{hGl_c^2}$
		$V^2 = \frac{-\beta\omega^2 + \sqrt{\beta^2\omega^4 + 4\alpha^4\omega^2 - 4\alpha^4\gamma\omega^4}}{2(1-\gamma\omega^2)}$	
		$\frac{d(V^2)}{d\omega} = \frac{\left[(-\beta\omega)\sqrt{\beta^2\omega^4 + 4\alpha^4\omega^2 - 4\alpha^4\gamma\omega^4} + (\beta^2\omega^3) + (2\alpha^4\omega)(1-\gamma\omega^2) \right]}{(1-\gamma\omega^2)^2 \sqrt{\beta^2\omega^4 + 4\alpha^4\omega^2 - 4\alpha^4\gamma\omega^4}}$	

*The thin beam (plate) results are a limiting case of the more general thick beam (plate) results and hence it is sufficient to work only with the thick beam (plate) equation over the full range of frequencies.

Table 3-3: Summary of Power Expressions

Structure	Loading	Power Expression
Beam (Thick or Thin)	Longitudinal	$P = \frac{F_o^2}{2A\sqrt{E\rho}}$
Plate (Thick or Thin)	Longitudinal	$P = \frac{F_o^2}{2A} \sqrt{\frac{1-\nu^2}{E\rho}}$
Beam (Thin)	Bending, Mid-Loading	$P = \frac{F_o^2}{8\sqrt{(\rho A)^3 EI \sqrt{\omega}}}$
	End Transverse Loading	$P = \frac{F_o^2}{2\sqrt{(\rho A)^3 EI \sqrt{\omega}}}$
Plate (Thin)	Bending, Mid-Loading	$P = \frac{F_o^2}{16} \sqrt{\frac{1-\nu^2}{EI' \rho h}}$
	End Transverse Loading	$P = \frac{F_o^2}{4.62} \sqrt{\frac{1-\nu^2}{EI' \rho h}}$
Beam (Thick)	Bending	$P = \frac{F_o^2}{2} [AB(B^2 + D^2)]^{\frac{1}{4}} \left[(B+C)\cos\frac{\theta}{2} + (B-C)\sin\frac{\theta}{2} \right]$ <p>where:</p> $A = \frac{k}{4\omega\rho A \sqrt{\left[1 - \left(\frac{E}{GK^2}\right)\left(\frac{k^4 h^4}{12}\right)\right]^2 + \left[\frac{E}{GK^2} + 1\right]^2 \left[\frac{k^4 h^4}{24}\right]^2}}$ $B = \sqrt{1 - \left(\frac{E}{GK^2}\right)\left(\frac{k^4 h^4}{144}\right)}$ $C = \left(\frac{E}{GK^2}\right)\left(\frac{k^2 h^2}{12}\right)$ $D = \left(\frac{E}{GK^2} + 1\right)\left(\frac{k^4 h^4}{12}\right)$ $\theta = \tan^{-1}\left(\frac{-D}{B}\right)$ $k = \left[\frac{EI}{\rho A \omega^2}\right]^{\frac{1}{4}}$
Plate (Thick)	Bending	$P = \left\{ \frac{F_o^2}{16} \sqrt{\frac{1-\nu^2}{\rho h EI'}} \right\} \frac{\left\{ 1 + \left(\frac{k^2 h^2}{24}\right)^2 \left(\frac{2E}{GK^2(1-\nu^2)}\right) \left(\frac{E}{GK^2(1-\nu^2)}\right) - 1 \right\}}{\left\{ 1 + \left(\frac{k^2 h^2}{24}\right)^2 \left(\frac{E}{GK^2(1-\nu^2)}\right) - 1 \right\}}$

3.2.2 Treatment of Junctions

A critical aspect within the Power Flow Finite Element Analysis is the modeling of the effects of junctions between structural members. In general, a wave incident on a junction will result in both reflected and transmitted waves, often of more than one type. As highlighted in Section 2, several studies were carried out to investigate the modeling of various types of junctions that occur in ship structures. Detailed descriptions of the treatment of junctions have been provided in several reports (see Burrell et al, 1991, 1992 a, b; Smith and Chernuka, 1996,1997). Only brief summary is provided here to highlight the treatment of junctions.

It has been shown that the transmission of energy across a junction is governed by the expression (Nefske and Sung, 1989):

$$q_{12} = -\tau(l_{c2}e_2 - l_{c1}e_1) \quad [3-4]$$

where: q_{12} = energy transferred across junction
 e_i = energy density on structure I
 l_{ci} = PFFEA energy conduction parameters
 τ = transmission efficiency $\left(\frac{\text{Transmitted Power}}{\text{Incident Power}}\right)$

Since $l_{ci}e_i$ is the dynamic variable in PFFEA, and q_{12} is the parameter we wish to determine, then what is required is to evaluate the transmission efficiency τ for each type of structure and wave type. Obviously it is impractical to determine the form of the transmission efficiency for every possible junction type and hence it is desired to develop one, or perhaps a few, general junctions which can be used with appropriate simplifications to represent all anticipated junctions.

To assist in the development of a general methodology, three areas of study were identified. The first is the investigation of wave propagation in grillages. The results are also applicable with some very minor modifications to junctions of plates in which the direction of the propagation is normal to the junction. The second area of study concerned waves intersecting plate junctions at oblique angles. The third aspect is the modeling of beam-stiffener junctions such as those that occur on rib-stiffened plates. For grillage structures, the theory was developed for (a) bending waves in the plane of the junction with the incoming wave being bending or longitudinal and (b) bending out-of-plane of the junction, with the in-coming wave being bending or torsion. Furthermore, the theory was also developed for oblique incidence where the law of refraction (Snell's law) was used to develop the equations for co-planar plates and plates at right angles with incoming wave being longitudinal or bending (Burrell et al., 1991).

The current junction modeling capabilities in SNAP follow the works of Smith and Chernuka (1996, 1997), which have refined and enhanced the capabilities developed

earlier. They developed junction stiffness matrices for beam-beam junctions (both Euler and Timoshenko beam), beam-plate, and plate-plate junctions. These junction stiffness matrices are treated as extremely generalized conductivity matrix terms.

Consider the case of fully dynamic Euler-Bernoulli beams with bending about two axes as well as axial and torsional motion. They give rise to four independently propagating wave modes: two bending, one longitudinal, and torsional. Each of these is capable of transmitting energy at a particular speed known as the group velocity, which is determined by the properties of the beam and the nature of the oscillation. Two additional wave modes, called evanescent waves or near-fields occur. They do not propagate energy unless the beam is quite short and the evanescent modes emanating from opposite ends of beams overlap. In typical beam-type structures vibrating at high frequency this is not a concern, and the influence of the evanescent modes on energy propagation along the beam can be neglected. But it is necessary to include the evanescent modes if the correct dynamic equilibrium of a junction is to be established.

The junctions considered consist of an arbitrary number of beams joined through their centroids at arbitrary angles in three dimensions. The beams themselves are assumed semi-infinite so that reflections from the remote ends can be excluded from the analysis. First, the kinematic and dynamic relationships for this type of beam are presented, and then the equations of compatibility and equilibrium are developed for the junction in the general case.

In Figure 3-1, a local coordinate system xyz is defined for a semi-infinite beam. Displacements u, v, w , and rotations $\theta_x, \theta_y, \theta_z$ describe the position and orientation of the cross-section as a function of x and time t . Longitudinal, flexural and torsional waves traveling in the x -direction causes the following displacements.

$$u(x, t) = \alpha_l e^{-i(k_l x - \omega t)} \quad [3-5]$$

$$v(x, t) = \left(\alpha_f^y e^{-ik_b^y x} + \alpha_n^y e^{-k_b^y x} \right) e^{i\omega t} \quad [3-6]$$

$$w(x, t) = \left(\alpha_f^z e^{-ik_b^z x} + \alpha_n^z e^{-k_b^z x} \right) e^{i\omega t} \quad [3-7]$$

$$\theta_x(x, t) = \alpha_t e^{-i(k_t x - \omega t)} \quad [3-8]$$

$$\theta_y(x, t) = -\frac{\partial w}{\partial x} = \left(ik_b^z \alpha_f^z e^{-k_b^z x} + k_b^z \alpha_n^z e^{-k_b^z x} \right) e^{i\omega t} \quad [3-9]$$

$$\theta_z(x, t) = \frac{\partial v}{\partial x} = -\left(ik_b^y \alpha_f^y e^{-k_b^y x} + k_b^y \alpha_n^y e^{-k_b^y x} \right) e^{i\omega t} \quad [3-10]$$

where:

α_l = complex amplitude of the axial wave

k_l = wave number of longitudinal vibration $\left(\omega \sqrt{\rho/E} \right)$

α_f^y, α_n^y = complex amplitude of x-y plane flexural amplitude of propagation (farfield)

and evanescent (near-field) wave components

α_f^z, α_n^z = complex amplitude of x-z plane flexural amplitude of propagation (farfield) and

evanescent (near-field) wave components

k_b^y = wave number of x-y plane flexural vibration $\left(\frac{\rho A \omega^2}{EI_z}\right)^{1/4}$

k_b^z = wave number of x-z plane flexural vibration $\left(\frac{\rho A \omega^2}{EI_y}\right)^{1/4}$

k_t = $\omega \sqrt{\rho I_p / GJ}$

A = Cross sectional area

I_y, I_z = Moment of inertial about y-z-axis respectively

I_{yp} = Polar moment of area

GJ = Terminal rigidity

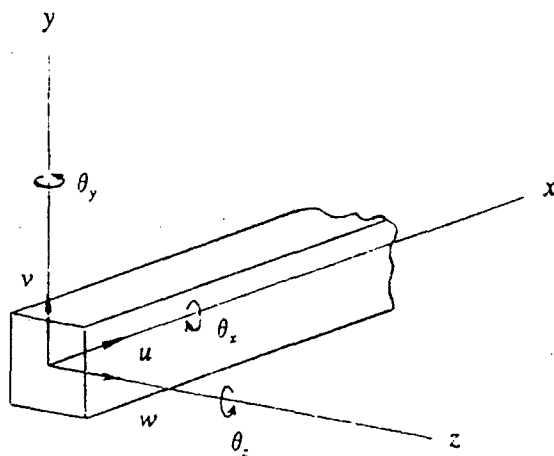


Figure 3-1: Local Co-ordinate System for Semi-Infinite Beam

By setting $x=0$ (at the junction) and dropping the common factor $e^{i\omega t}$, the above expressions can be written in matrix form as

$$u_o = \begin{Bmatrix} u \\ v \\ w \\ \theta_x \\ \theta_y \\ \theta_z \end{Bmatrix}_o = \begin{bmatrix} 1 & 0 & 0 & 0 & 0 & 0 \\ 0 & 1 & 0 & 0 & 0 & 1 \\ 0 & 0 & 1 & 0 & 1 & 0 \\ 0 & 0 & 0 & 1 & 0 & 0 \\ 0 & 0 & ik_b^z & 0 & k_b^z & 0 \\ 0 & -ik_b^y & 0 & 0 & 0 & -k_b^y \end{bmatrix} \begin{Bmatrix} \alpha_l \\ \alpha_f^y \\ \alpha_f^z \\ \alpha_t \\ \alpha_n^z \\ \alpha_n^y \end{Bmatrix} \quad [3-11]$$

Or alternatively

$$u_o = D\alpha \quad [3-12]$$

Similarly, the force vector can be written in matrix form as

$$f_o = \begin{Bmatrix} f_x \\ V_y \\ V_z \\ m_x \\ m_y \\ m_z \end{Bmatrix}_o = \begin{bmatrix} ik_t EA & 0 & 0 & 0 & 0 & 0 \\ 0 & i(k_b^y)^3 EI_z & 0 & 0 & 0 & -(k_b^y)^3 EI_z \\ 0 & 0 & i(k_b^z)^3 EI_y & 0 & -(k_b^z)^3 EI_y & 0 \\ 0 & 0 & 0 & ik_t GJ & 0 & 0 \\ 0 & 0 & -(k_b^z)^2 EI_y & 0 & (k_b^z)^2 EI_y & 0 \\ 0 & (k_b^y)^2 EI_z & 0 & 0 & 0 & -(k_b^y)^2 EI_z \end{bmatrix} \begin{Bmatrix} \alpha_l \\ \alpha_f^y \\ \alpha_f^z \\ \alpha_t \\ \alpha_n^z \\ \alpha_n^y \end{Bmatrix} \quad [3-13]$$

Or in complex for

$$f_o = B\alpha \quad [3-14]$$

Eliminating the transmission coefficients α , we obtain the force vector in terms of the displacement vector:

$$f_o = \kappa u_o \quad [3-15]$$

where $\kappa = BD^{-1}$

$$\kappa = \begin{bmatrix} ik_t EA & 0 & 0 & 0 & 0 & 0 \\ 0 & (i-1)(k_b^y)^3 EI_z & 0 & 0 & 0 & i(k_b^y)^3 EI_z \\ 0 & 0 & (i-1)(k_b^z)^3 EI_y & 0 & -i(k_b^z)^3 EI_y & 0 \\ 0 & 0 & 0 & ik_t GJ & 0 & 0 \\ 0 & 0 & -i(k_b^z)^2 EI_y & 0 & (i+1)(k_b^z)^2 EI_y & 0 \\ 0 & i(k_b^y)^2 EI_z & 0 & 0 & 0 & -(i+1)(k_b^y)^2 EI_z \end{bmatrix} \quad [3-16]$$

is a 6x6 symmetric matrix of semi-infinite beam as seen from the junction.

The stiffness matrices in local co-ordinates can be transformed to obtain the global stiffness matrix of the junction as

$$K_j = \sum_{i=1}^n T_i^T K_i T_i \quad [3-17]$$

where

n = number of beams meeting at joint

T_i = transformation matrix for beam $i = \text{diag}\{A, A\}$

$$A = \begin{bmatrix} \cos\psi \cos\phi - \cos\theta \sin\phi \sin\psi & \cos\psi \sin\phi + \cos\theta \cos\phi \sin\psi & \sin\theta \sin\psi \\ -\sin\psi \cos\phi - \cos\theta \sin\phi \cos\psi & -\sin\psi \sin\phi + \cos\theta \cos\phi \cos\psi & \sin\theta \cos\psi \\ \sin\theta \sin\phi & -\sin\theta \cos\phi & \cos\theta \end{bmatrix}$$

where ϕ, θ, ψ are the Euler angles between the local and global coordinate systems. Expressions for Timoshenko beams, beam-plate and plate-plate junctions are similarly derived. (Smith and Chernuka, 1996, 1997)

3.2.3 Fluid Modelling

Smith and Chernuka (1996) presented basic formulations of power flow models for fluid-loaded plates with fluid loading on one side of an infinite plate. The dispersion relation for plane waves is altered such that two distinct frequency ranges are established. In the low frequency range, the bending wavelength of the plate is less than the wavelength in the fluid. Flexural plate vibrations cannot effectively radiate energy to the fluid in this case but kinetic energy is imparted to the fluid, causing mass loading on the plate. The mass loading reduces the phase velocity of the plate waves by an amount, which can be accurately predicted, but there is no change to the effective loss factor. In the high-frequency range, the structural wavelength is longer than the fluid factor for the plate, which can be estimated from the radiation efficiency. The phase speed of the plate waves becomes invariant with frequency at a value identical to the wave speed in the fluid.

The frequency separating these two fundamentally different zones is called the critical frequency and is defined as the frequency at which the wavelengths in the fluid and the plate are the same. Denoting the critical frequency as f_c ,

$$f_c = \frac{c_w^2}{2\pi} \left(\frac{m}{D} \right)^{1/2} \quad [3-19]$$

where c_w is the wave speed in the fluid, m is the mass per unit area of the plate and D is its flexural rigidity. For steel plates in water $f_c = 218/t$, where t is the thickness in meters. This result is not far below the upper frequency limit for thin plate theory $f = 272/t$ Hz, and because of this, Junger and Feit (1986) noted that it is advisable to include shear deformation in the plate formulation for frequencies above f_c . The high frequency range will be important only for relatively thick plates (e.g. for 1" thick plates, $f_c = 8600$ Hz). Most analysis of thin plates will be conducted in the low frequency range where the effect of the fluid is purely inertial.

To construct an appropriate power flow model, it is sufficient to employ the two-dimensional diffuse equations (3-1 and 3-2) in which the group velocity c and loss factor η have been adjusted for the presence of the fluid. Note that only the flexural energy modes of the plate need to be adjusted, as the in-plane wave modes are assumed unaffected by the fluid loading. Below the critical frequency, the group velocity can be obtained from the dispersion relation given by Junger and Feit for the single propagating root of the fluid loaded plate:

$$k^4 = k_B^4 \left[1 + \frac{\rho_w}{m \sqrt{k^2 - k_w^2}} \right] \quad [3-20]$$

where k is the propagation constant for the fluid-loaded plate ρ_w and k_w the density and wave number of the fluid, and m and k_B are the mass per unit area and wave number of the free plate. Differentiating the dispersion relation (Equation 3-20) with respect to frequency and isolating the term $\partial\omega/\partial k$ leads to an expression for the group velocity.

For fluid-loaded plates subjected to harmonic forces and it is found that power may be lost to the fluid in both the sub- and super-critical ranges.

Fluid-loading affects the input power from an external excitation in two ways: (i) by changes to the driving point admittance caused by the added mass of the fluid; and (ii) by power lost directly to the fluid from the driving point. Taking as an example a simple harmonic point force acting on an infinite plate, the driving point admittance in the presence of fluid loading is,

$$Y_f = Y_o \frac{4}{5} \left(m \frac{k_B}{\rho_w} \right)^{2/5} \left(1 - i \tan \frac{\pi}{10} \right) \quad [3-21]$$

where Y_o is the real, driving point admittance of a free, infinite plate. The input power is proportional to the real part of Y_f , which can be seen to be somewhat less than the free plate value in the sub-critical range.

The effective input power to a plate is further reduced by radiation to the fluid from the driving point. This type of radiation is the result of interaction between the near field adjacent to the driving point and the surrounding fluid. Again considering a simple harmonic point force of amplitude F on an infinite plate, the power radiated to the fluid from the driving point depends on the degree of fluid loading. Defining the parameter $\beta = \rho_w c_w / m \omega$, the radiated power is found to be

$$P_r = \frac{k^2 \beta^2 |F|^2}{4\pi \rho_w c_w} \quad \beta \ll 1 \quad [3-22]$$

$$P_r = \frac{k^2 |F|^2}{12\pi \rho_w c_w} \quad \beta \gg 1 \quad [3-23]$$

The first case is for when the fluid-loading is light and is relevant to high frequencies and thick plates. The second case is for heavy fluid loading or low frequencies and thin plates. The plate properties play no role in the latter result as the mass of the plate is negligible in comparison to the fluid. The radiated power in (Equation 3-22 and 3-23) must be subtracted from the input power computed using the adjusted driving-point admittance. Further development of the models was suggested by Smith and Chernuka (1996).

4. VALIDATION of SNAP

SNAP has been validated through a series of example problems. The validation models investigated in this chapter range from a simple beam to a complex stiffened panel structure.

4.1 Simple Beam (Flexural Loading)

The simple beam, illustrated in Figure 4-1, is used to validate PFFE calculations for beam structures. The beam is harmonically loaded with a 1000N load (RMS value) applied to the center. Model parameters are displayed in Table 4-1.

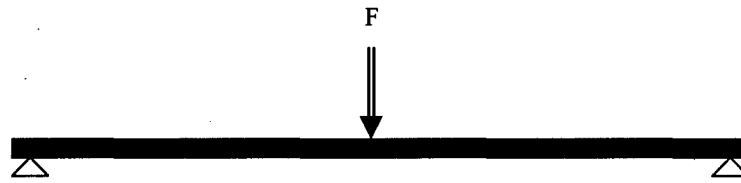


Figure 4-1: Model of a Simple Beam (Flexural Load)

Table 4-1: Model Parameters for a Simple Beam (Flexural Load)

Length	1.165 m
Height	0.01 m
Width	0.05 m
Density	8000 kg/m ³
Young's Modulus	2.0 x 10 ¹¹ N/m ²
Loss Factor	0.2
Mass	4.66 kg
Fundamental Frequency	16.7 Hz

ANSYS results, from Smith (1997), are used to validate VASTF at a frequency of 10000Hz. Temperature and displacement comparisons are shown in Figure 4-2 and Figure -3, respectively. The two Finite Element (FE) packages produce very similar results.

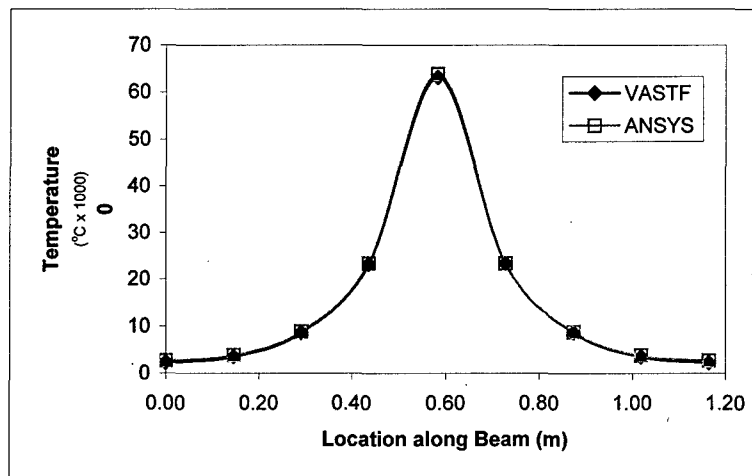


Figure 4-2: Temperature Results for Beam Test Problem (VASTF and ANSYS)

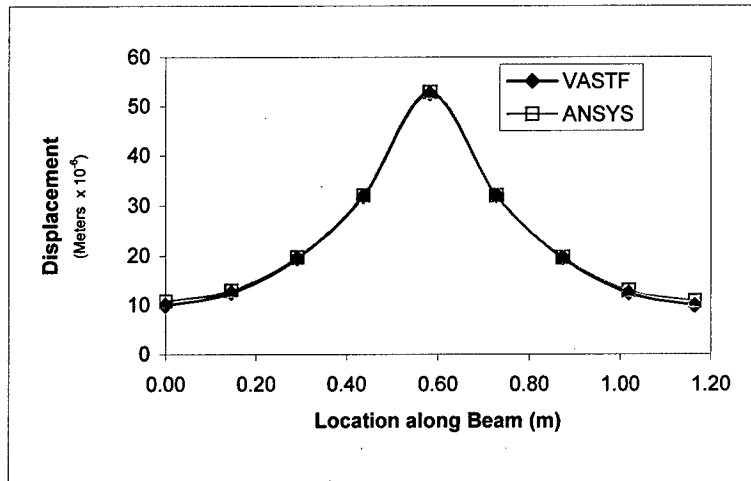


Figure 4-3: Non-Dimensional Displacement Results for Beam Test Problem (VASTF and ANSYS)

Burrell (1989) uses another approach called the modal method for validation purposes. Burrell (1989) states that the modal method provides correct results for this beam model within the scope of this problem, therefore is used as a datum for this analysis. Two PFEA models are developed, one using beam elements and a second using four node quadrilateral shell elements. Results are summarized in Figure 4-4. Note that displacement in decibels is found by:

$$u_{dB} = 20 \log(u_{no\ dim}) \quad [4-1]$$

where

$$u_{dB} = \text{Displacement (dB)}$$

$$u_{no\ dim} = \frac{M\omega_n u}{F}, \text{ non-dimensional displacement}$$

$$M = \text{Mass (Kg)}$$

$$\omega_n = \text{Angular Natural Frequency (s}^{-1}\text{)}$$

$$u = \text{displacement (m)}$$

$$F = \text{RMS load value}$$

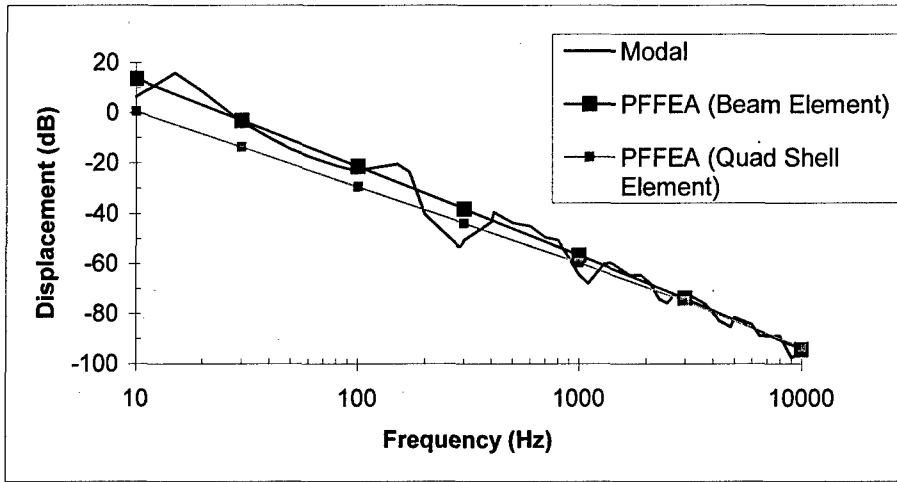


Figure 4-4: Displacement Results (at L/4) for a Harmonically Loaded Beam (Modal and PFFEA)

4.2 Cantilever Beam (Axial Loading)

The cantilever beam, illustrated in Figure 4-5 is axially loaded with a harmonic load of 1000N (RMS value). Model parameters are displayed in Table 4-2.



Figure 4-5: Cantilever Beam (Axial Load)

Table 4-2: Model Parameters for a Cantilever Beam (Axial Load)

Length	1.165 m
Height	0.01 m
Width	0.05 m
Density	8000 kg/m ³
Young's Modulus	2.0 x 10 ¹¹ N/m ²
Loss Factor	0.2
Mass	4.66 kg
Fundamental Frequency	1073 Hz

Temperature results along the beam at various frequencies are given in Figure 4-6. Burrell et al. (1992b) examined this exact problem and found the same results. Burrell et al. (1992b) also presented displacement results using analytical and SEA solution methods. The PFFEA solution is found to produce comparable results (Figure 4-7 and Figure 4-8). Note that the decibel unit and non-dimensionalizing is found using equation (4-1).

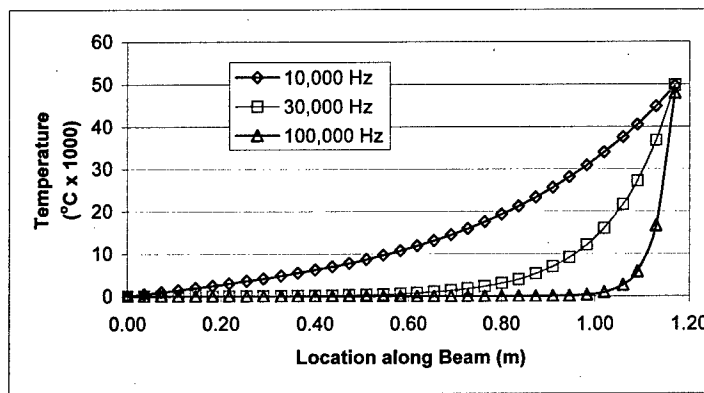


Figure 4-6: Temperature Results for a Cantilever Beam

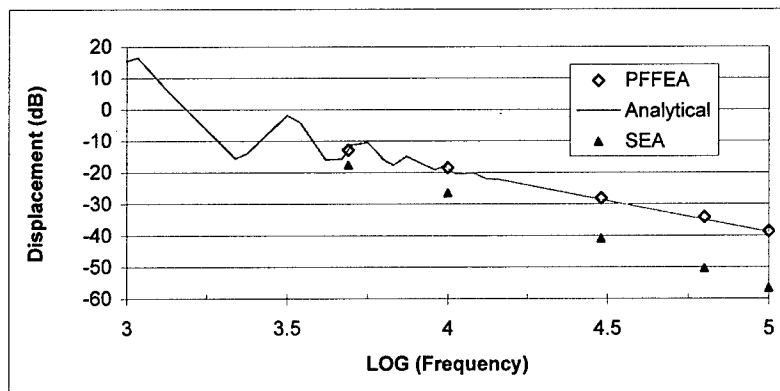
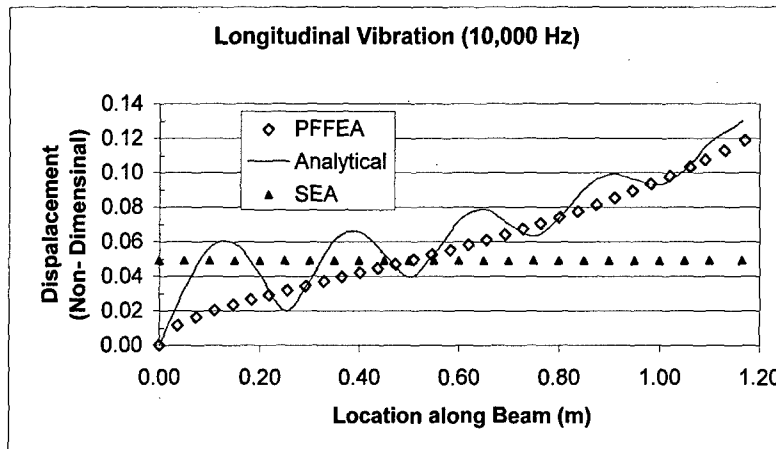
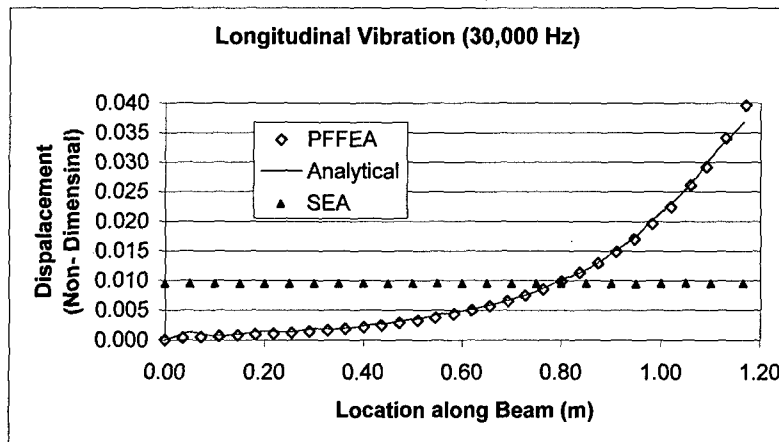


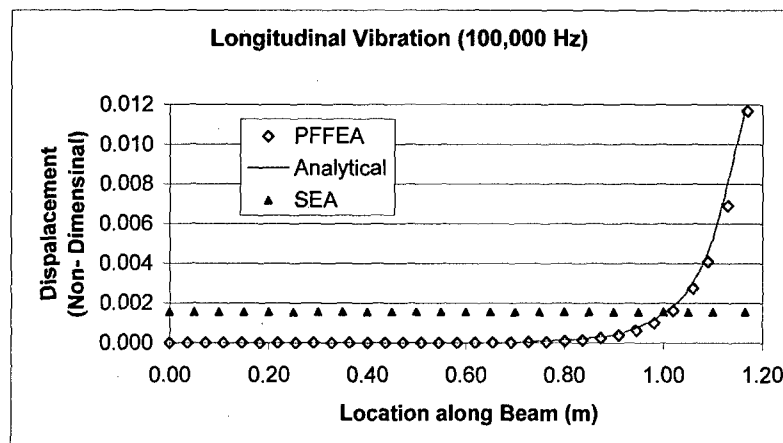
Figure 4-7: Frequency Vs Displacement (at loading location) for a Cantilever Beam Analyzed using PFFEA, Analytical and SEA Solutions



(A)



(B)



(C)

Figure 4-8: Non-Dimensional Displacement for a Cantilever using PFFEA, Analytical and SEA Solutions (A) 10,000Hz (B) 30,000Hz (C) 100,000Hz

4.3 Two Coupled Beams With Boundary Conditions

Two coupled beams, simply supported at three locations (Figure 4-9), are used to investigate the impact of boundary conditions on junctions. The first beam is harmonically loaded with a 1000N load (RMS value) applied to the center. Model parameters are displayed in Table 4-3.



Figure 4-9: Model of Two Coupled Beams (Flexural Load)

Table 4-3: Model Parameters for a Simple Beam (Flexural Load)

Length	2.330 m
Height	0.01 m
Width	0.05 m
Density	8000 kg/m ³
Young's Modulus	2.0 x10 ¹¹ N/m ²
Loss Factor	0.2
Mass	4.66 kg
Fundamental Frequency	16.7 Hz

This model, analyzed at a frequency of 1,000 Hz, produces a continuous displacement result as displayed in Figure 4-10. Nefske and Sung (1989) analyzed the same model and found a discontinuity in displacement at the middle constraint. Nefske and Sung (1989) explains that this discontinuity occurs because the middle constraint restricts energy flow between the two beams. The model in Figure 4-9 is then analyzed again without any boundary conditions, which produced the same results as displayed in Figure 4-10. The model analyzed with and without boundary conditions produces the same result, therefore proving that boundary conditions have not been implemented (for beam models) within the current version of the SNAP program.

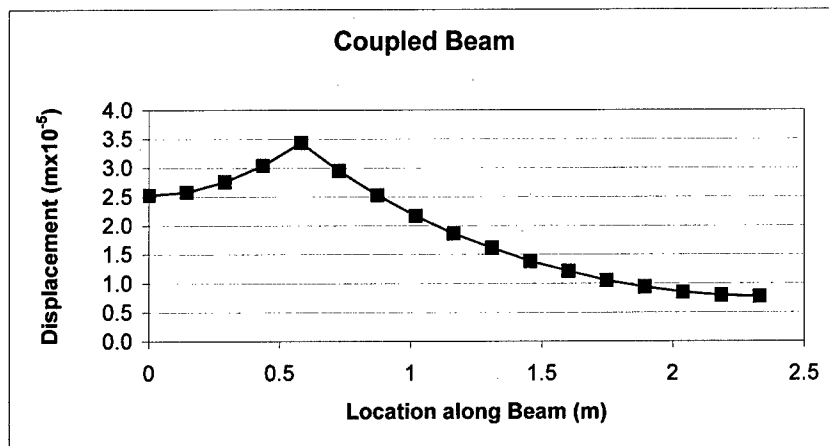


Figure 4-10: Displacement Results for a Coupled Beam

4.4 General Square Plate

A square plate, shown in Figure 4-11, is harmonically loaded with a unit load (RMS value) applied at the center. The 1m x 1m square plate is 1mm thick and is made with steel. Smith (1997) investigated this model using the standard conductivity method, which is used as a reference to validate our PFFEA model. Results are shown in the form of velocity amplitudes using various loss factors and a frequency of 700 Hz (Figure 4-12). Frequency response using various loss factors is shown in Figure 4-13. Note that the natural frequency of the plate is 4.754 Hz and that the decibel unit is found using equation 4-1.

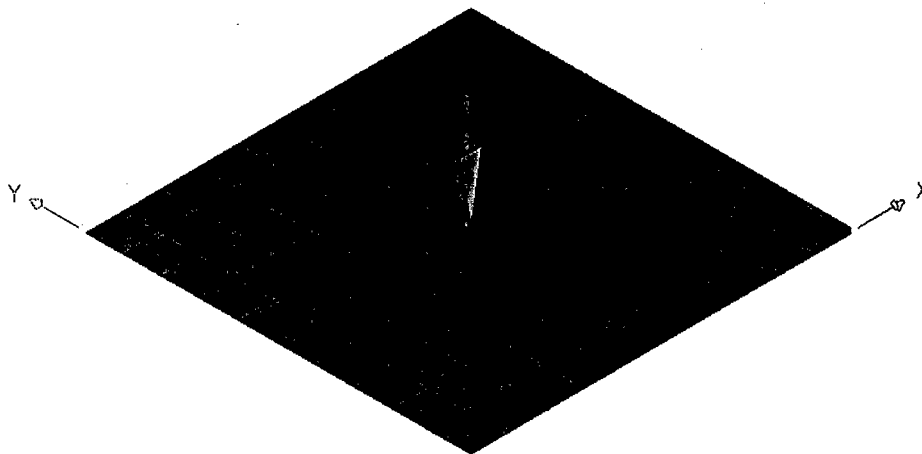
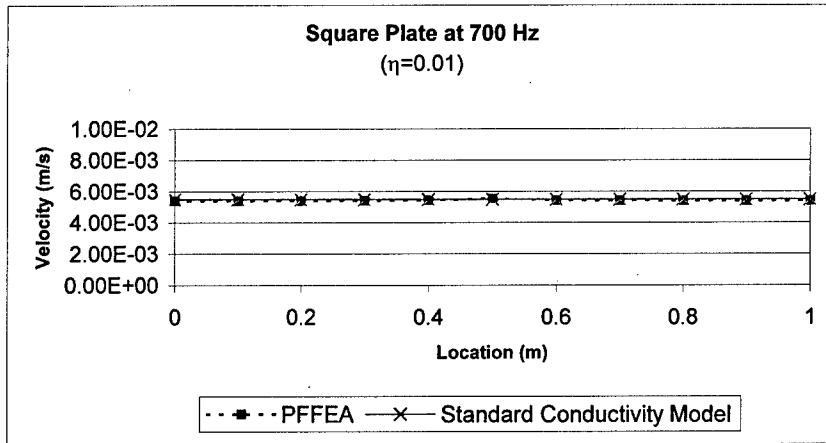
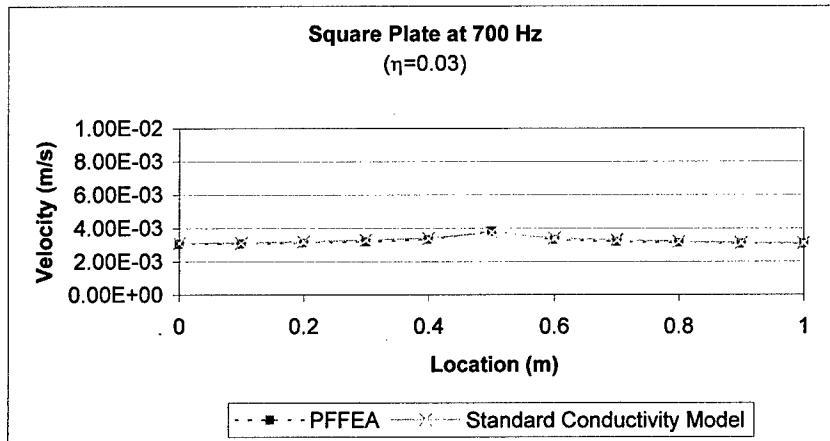


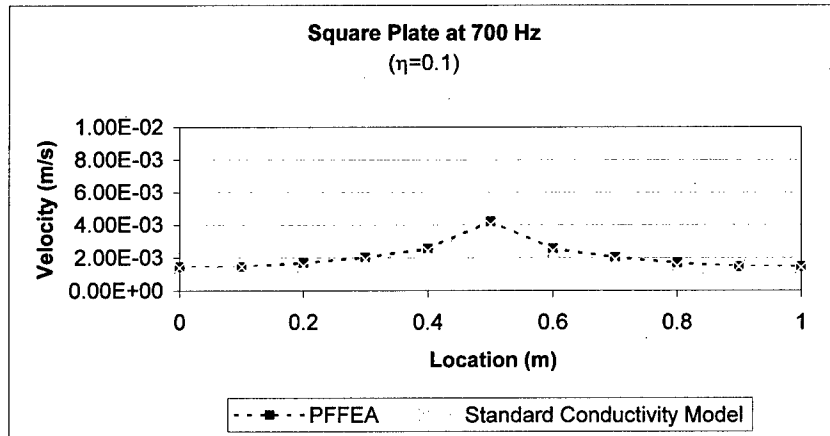
Figure 4-11: Model of a Square Plate



(A)

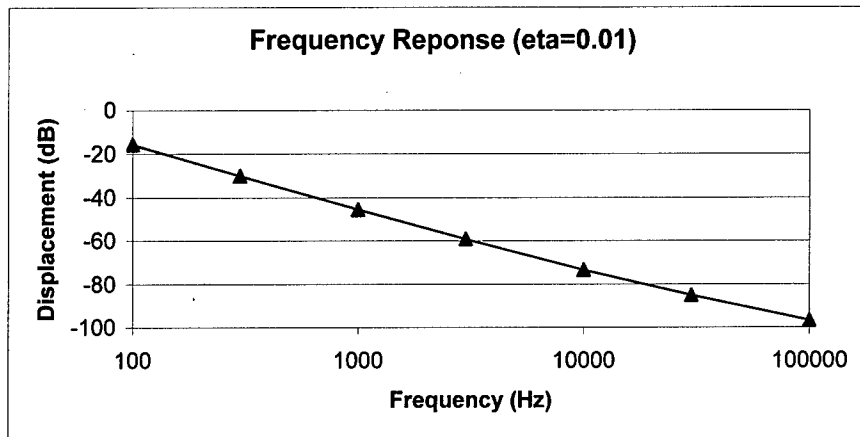


(B)

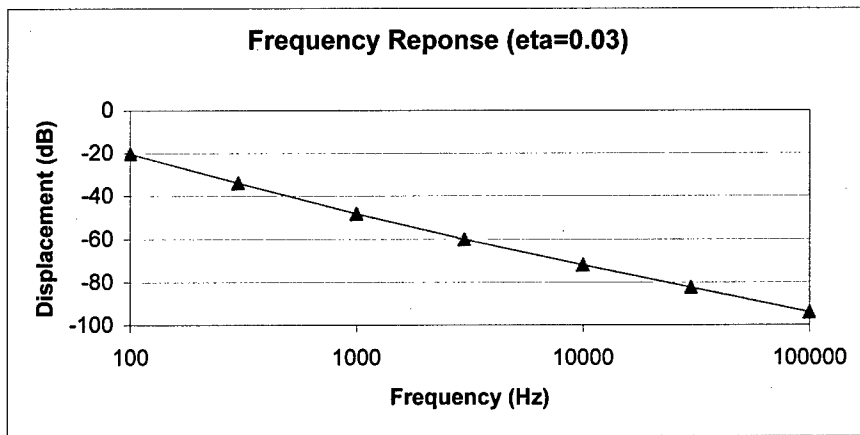


(C)

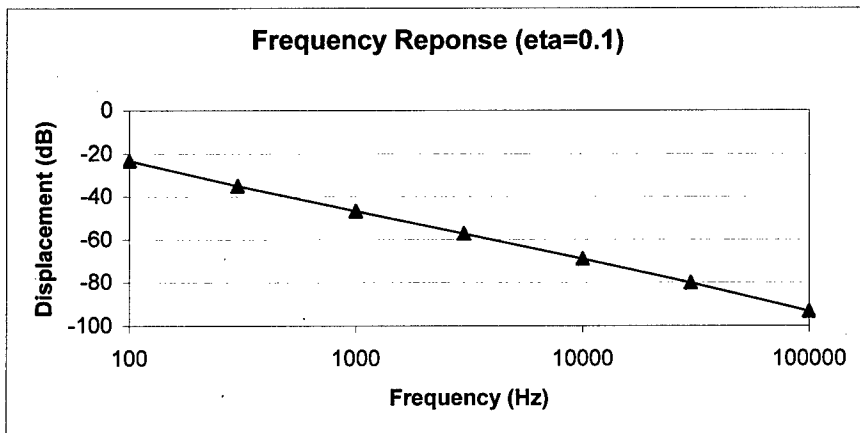
Figure 4-12: Velocity Amplitude (m/s) Along an Axis Passing Through the Center of a Square Plate, with Harmonic Excitation (A) $\eta=0.01$; (B) $\eta=0.03$; (C) $\eta=0.1$



(A)



(B)



(C)

Figure 4-13: Frequency Response of a 1m Square Plate Measured at the Center of the Plate, Where the Load is Applied A) eta=0.01; B) eta=0.03; C) eta=0.30

4.5 Rectangular Plate

A rectangular plate, measuring 1m x 0.5m x 1mm (Figure 4-14), is harmonically loaded with a 1000N peak amplitude load (i.e. 707N RMS load value) applied to the center. The steel plate has a natural frequency of 11.88Hz, and a loss factor of 0.01 is used in the analysis. Analytical and SEA results presented by Burrell et al. (1992b) for this rectangular plate are used as a reference to validate the plate model (Figure 4-15 and Figure 4-16).

Note that displacement in decibels is found by:

$$u_{dB} = 20\log(u_{no\ dim}) \quad [4-2]$$

where

u_{dB} = Displacement (dB)

$u_{no\ dim} = \frac{M\omega_n u}{F_o}$, non-dimensional displacement

M = Mass (Kg)

ω_n = Angular Natural Frequency (s^{-1})

u = displacement (m)

F_o = Peak Amplitude load value (RMS load * $\sqrt{2}$)

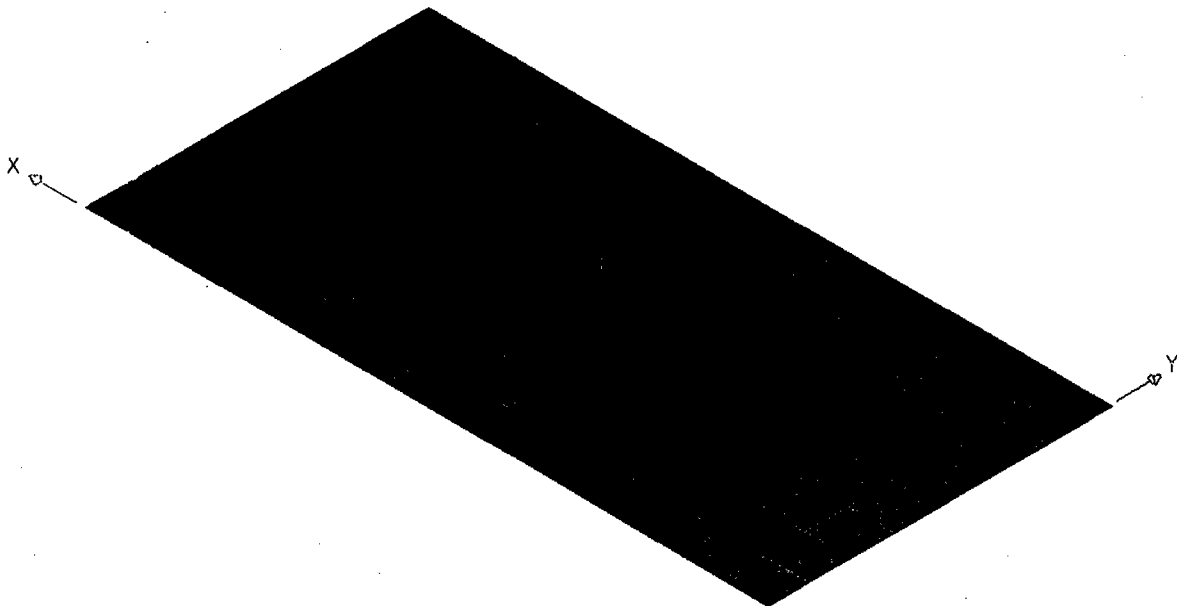


Figure 4-14: Model of a Rectangular Plate

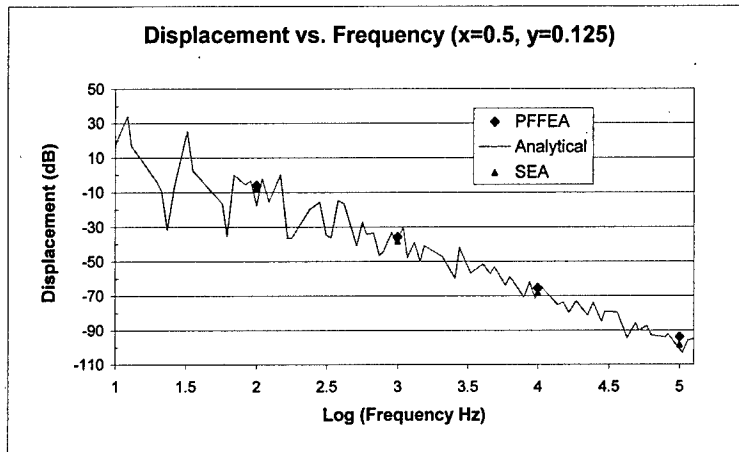
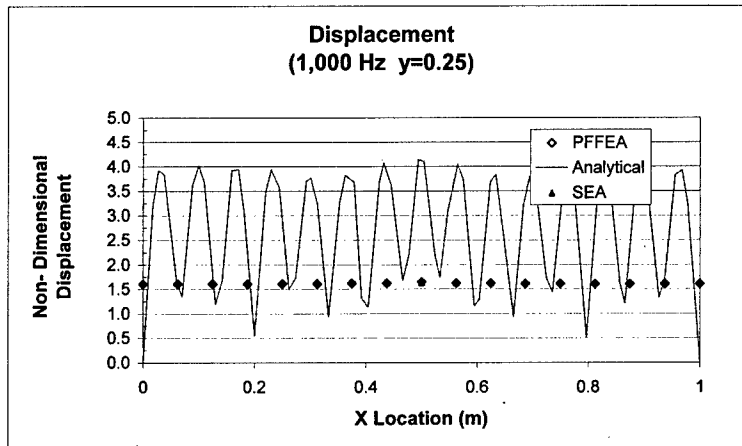
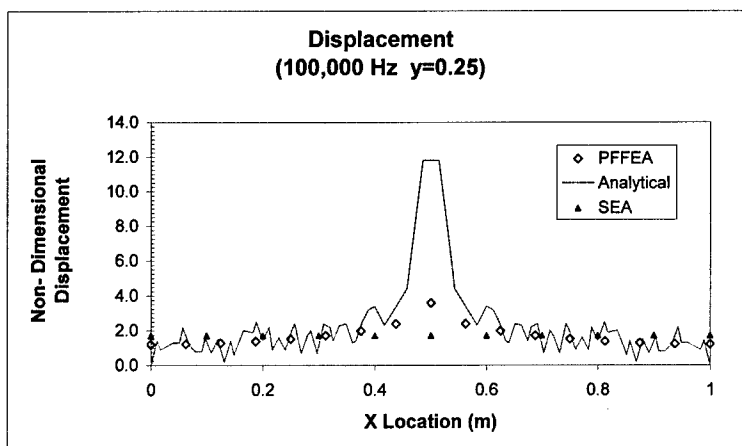


Figure 4-15: Rectangular Plate vs. Frequency



(A)



(B)

Figure 4-16: Rectangular Plate Vs. Location along the Plate Center A) 1,000Hz; B) 100,000Hz

4.6 Two Rectangular Beams at Right Angles (Flexural Load)

Two identical beams at right angles are harmonically loaded with a 1000N load (Peak Amplitude Load) applied to the center, as shown in Figure 4-17. Model parameters for each beam are displayed in Table 4-4. Flexural and Longitudinal results (at 10,000Hz) may be found for the source beam (externally loaded beam) and the receiving beam (no external load) in Figure 4-18. Note that the SEA results in Figure 4-18 are from Burrell et al. (1992).

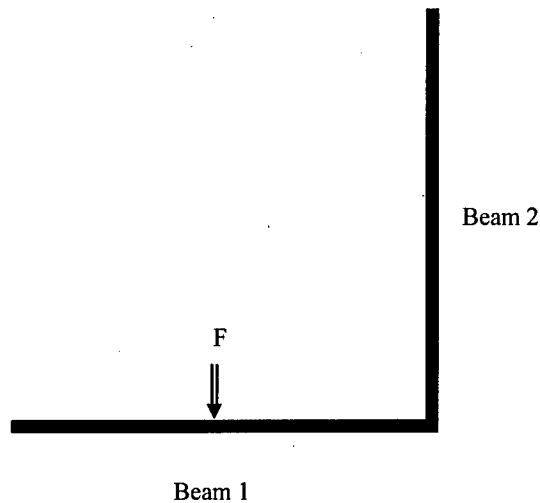
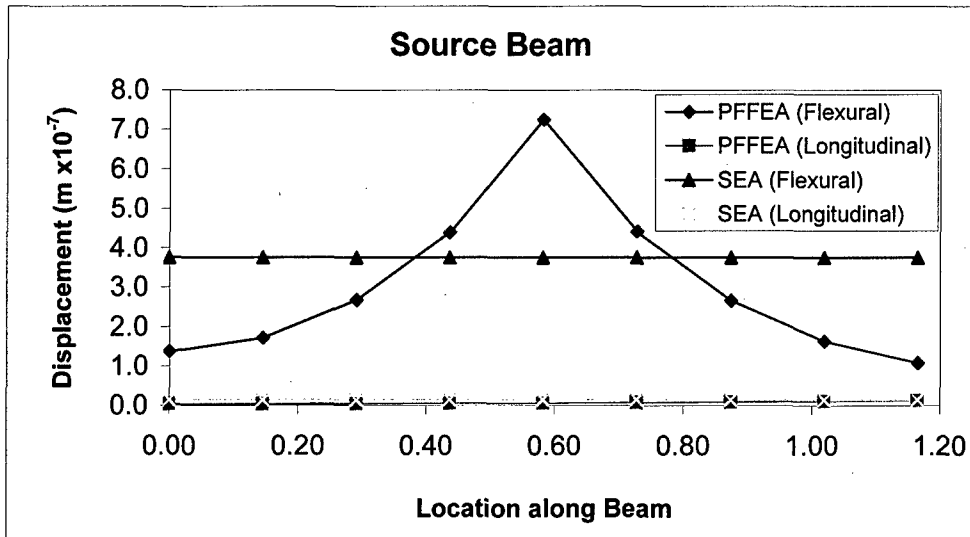


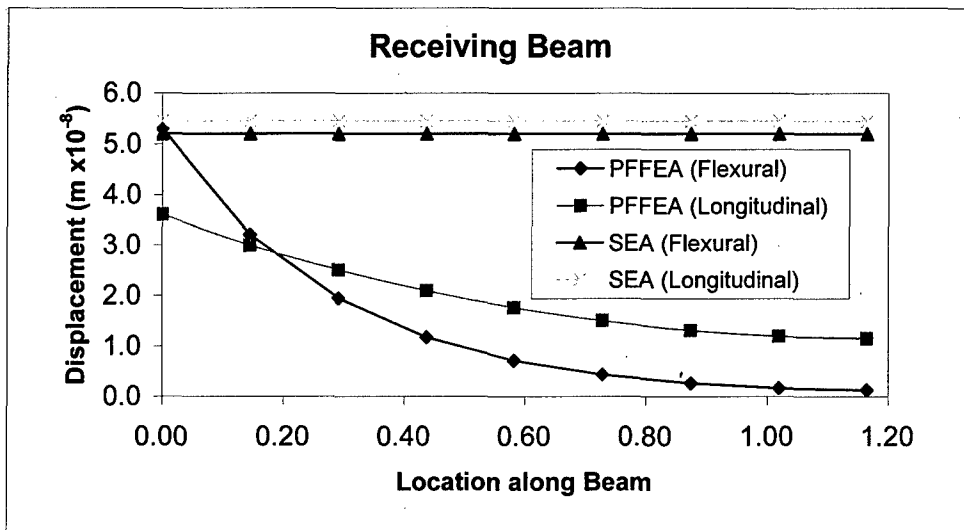
Figure 4-17: Model of Two Beams at Right Angles (Flexural Load)

Table 4-4: Model Parameters for a Simple Beam (Flexural Load)

Length	1.165 m
Height	0.01 m
Width	0.05 m
Density	8000 kg/m ³
Young's Modulus	2.0 x10 ¹¹ N/m ²
Loss Factor	0.2
Mass	4.66 kg
Fundamental Frequency	16.7 Hz



(A)

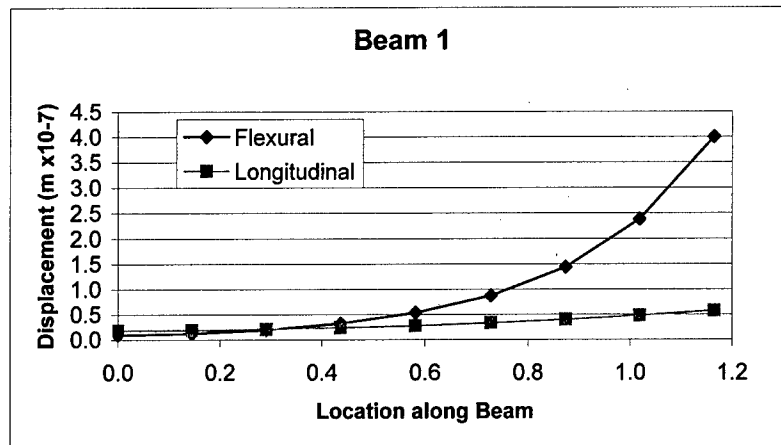


(B)

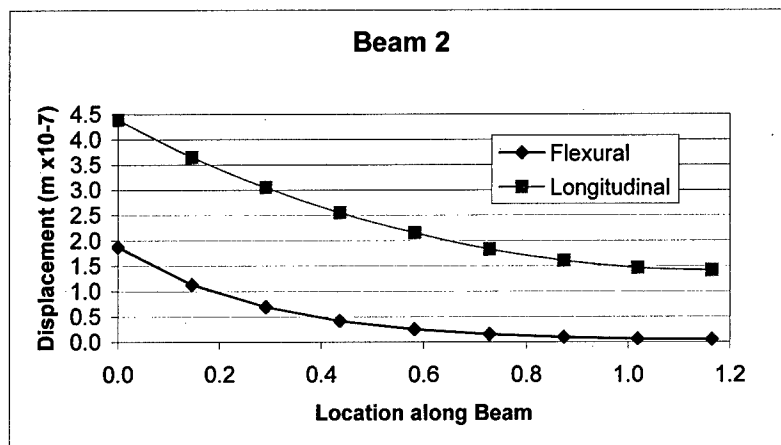
Figure 4-18: Displacement Results for Two Beams At Right Angles (A) Source Beam (B) Receiving Beam

4.7 Two Rectangular Beams at Right Angles (Axial Load)

This section investigates the same beam described in Figure 4-17 and Table 4-4 but moves the load to the beam intersection therefore causing beam 2 to be axially loaded. Results for this model (at 10,000Hz) are displayed in Figure 4-19.



(A)



(B)

Figure 4-19: PFFEA Displacement Results for Two Beams At Right Angles: (A) Source Beam (B) Receiving Beam

4.8 Two Rectangular Plates at Right Angles (Flexural Load)

Two rectangular plates with dimensions described in section 4.5 are loaded with a harmonic load of 1000N load (Peak Amplitude Load) applied to the center, as shown in Figure 4-20. Flexural and Longitudinal results (at 10,000Hz) may be found for the source beam (externally loaded beam) and the receiving beam (no external load) in Figure 4-21. Note that the SEA results in Figure 4-21 are from Burrell et al. (1992).

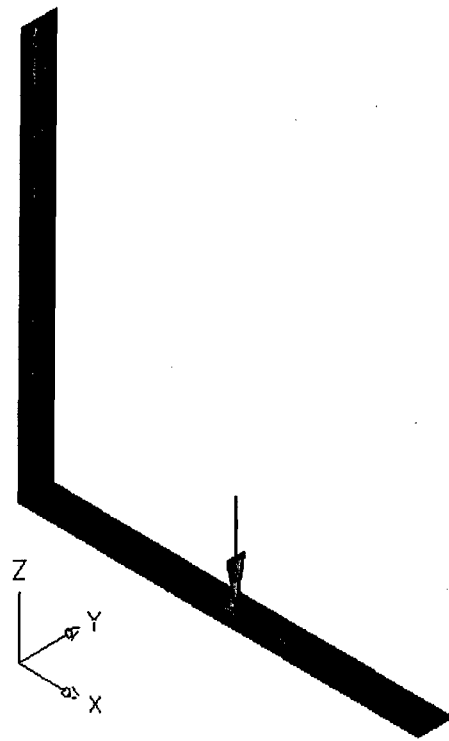
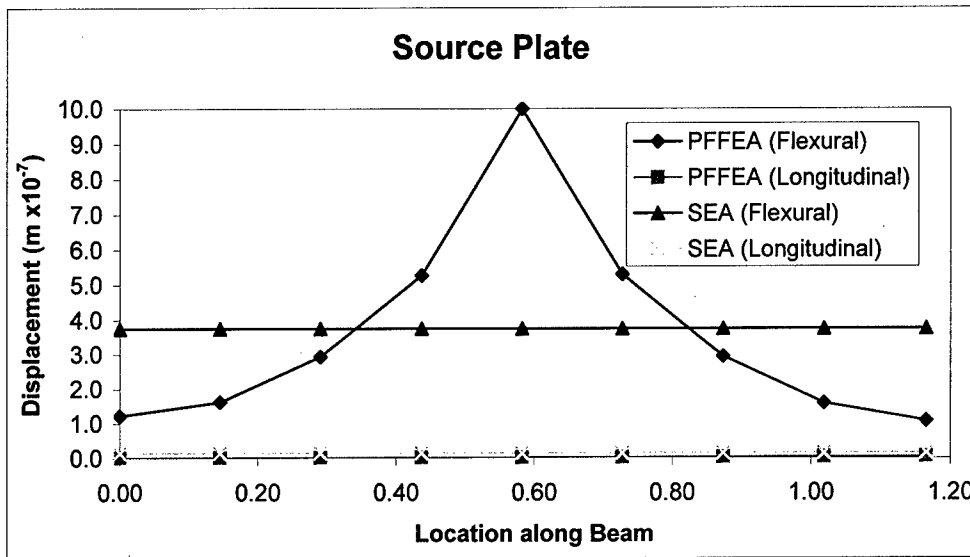
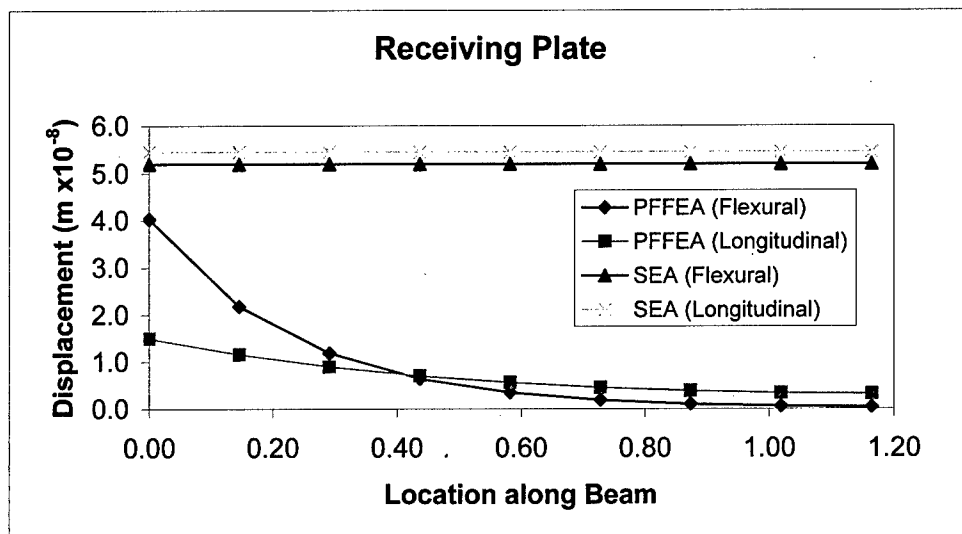


Figure 4-20: Model of Two Plates at Right Angles (Flexural Load)



(A)



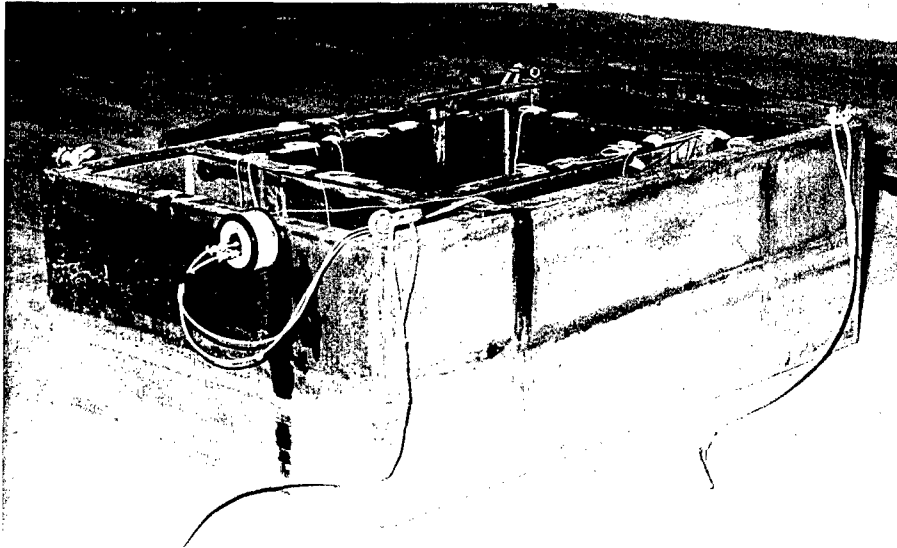
(B)

Figure 4-21: Displacement Results for Two Plates At Right Angles (A) Source Beam (B) Receiving Beam

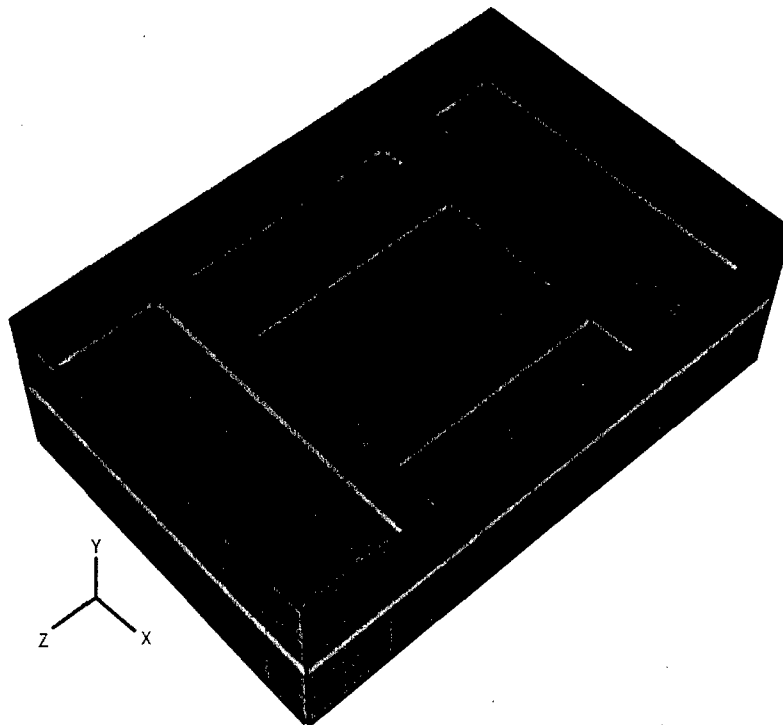
4.9 Stiffened Box Structure

A complex ship tank, depicted in Figure 4-22, is experimentally investigated at high frequencies (Smith and Brennan, 1998) at DRDC Atlantic and is used to validate PFFEA results. The reinforced steel tank is 1.83m long, 1.22m wide and 0.61m deep, with an inner compartment measuring 0.91m long, 0.61m wide and 0.61m deep. The vertical surfaces are stiffened with 6.4mm x 50.8mm bars depicted by thick red lines in Figure 4-

22. Each panel is made from 6.4mm thick mild steel, with the exception of the bottom of the inner compartment, which is 3.2mm thick. Numerical simulations were conducted for a total of four different loading scenarios (Figure 4-23A) and results were presented for two different plate locations (Figure 4-23B).



(A)



(B)

Figure 4-22: Stiffened Box Structure (A) Physical Structure (B) PFEA Model

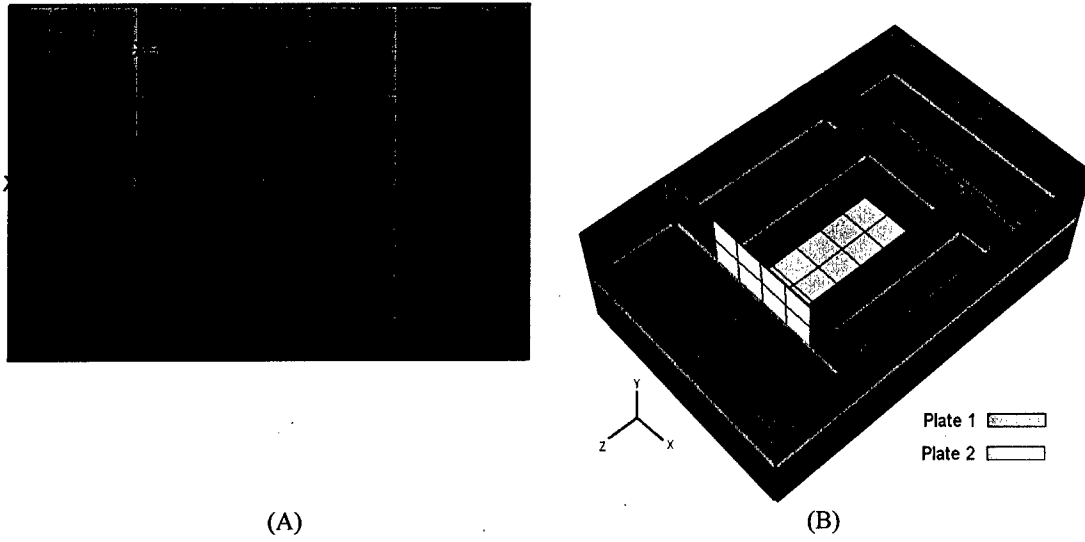


Figure 4-23: Stiffened Box Structure Parameters (A) Driving Points (B) Results are Reported on Plate Locations 1 and 2

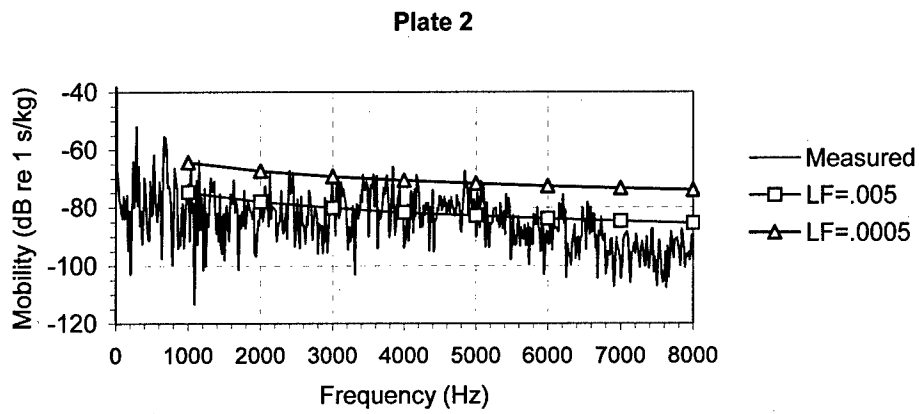
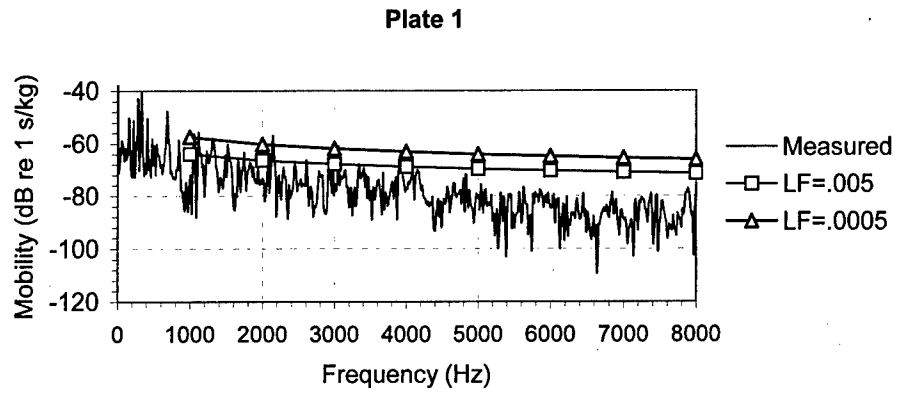
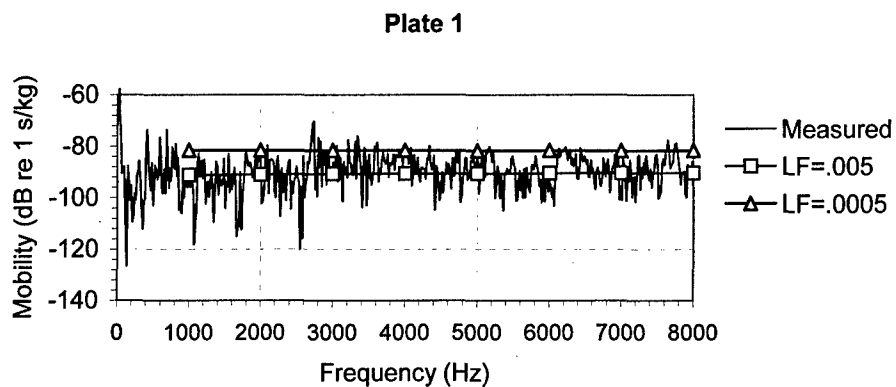
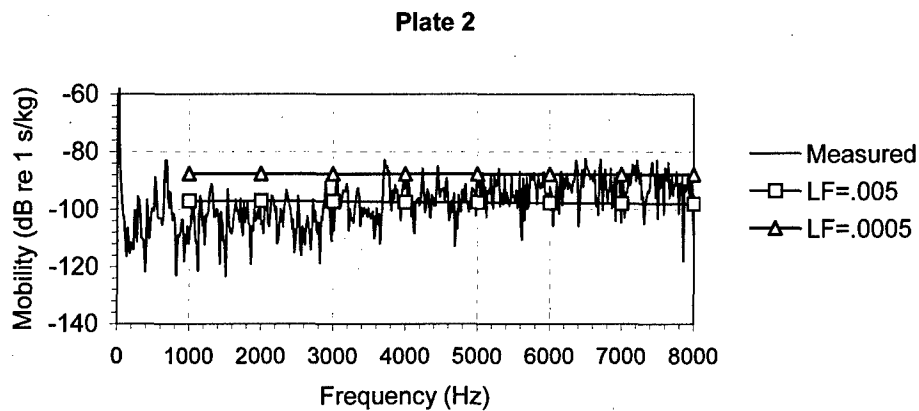


Figure 4-24: Mobility Results for Driving Point 1 (A) Plate 1 (B) Plate 2

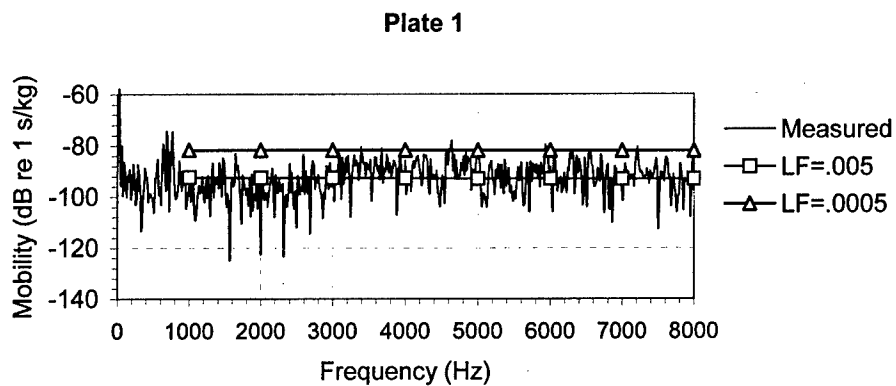


(A)

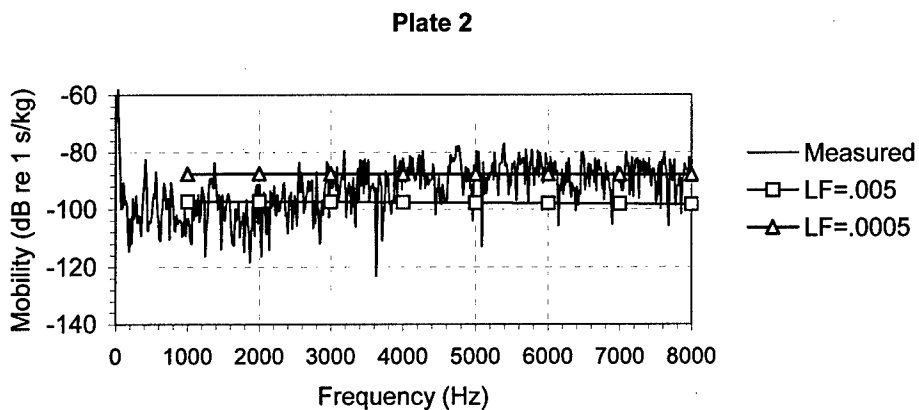


(B)

Figure 4-25: Mobility Results for Driving Point 2 (A) Plate 1 (B) Plate 2



(A)



(B)

Figure 4-26: Mobility Results for Driving Point 3 (A) Plate 1 (B) Plate 2

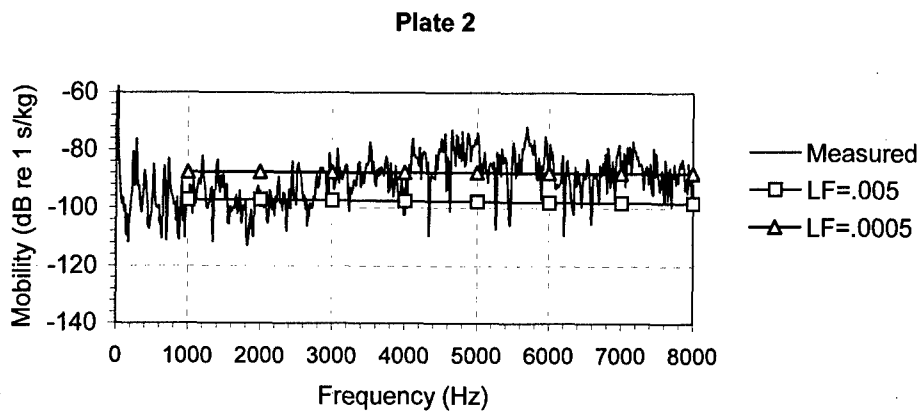
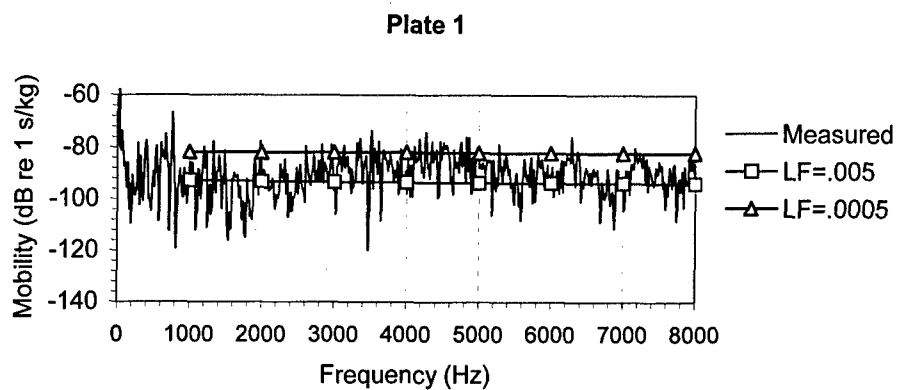


Figure 4-27: Mobility Results for Driving Point 4 (A) Plate 1 (B) Plate 2

5. TRANSIENT ENERGY FINITE ELEMENT ANALYSIS CAPABILITY

The basic formulation for energy finite element analysis (EFEA) is presented in Nefske and Sung (1989) (Equation 3-2). This formulation is derived via an analogy between statistical energy analysis (SEA) and FE-based heat conduction models. Details of this analogy have been presented in Section 3. It should be noted that the EFEA formulation model presented in Equation 3-2 is basically a transient model, since it includes the time varying term $\frac{\partial e}{\partial t}$. However, all the applications of EFEA that have been reported to date have implemented only steady state models, which may be obtained by simply neglecting the time varying component of Equation 3-2, $\frac{\partial e}{\partial t}$.

The purpose of the current task is to examine how to include transient capability in EFEA software. In order to facilitate this task, a review of transient modeling capabilities that have been implemented for EFEA has been undertaken, the results of which suggest that only limited work has been reported in this area. However, since EFEA is derived from SEA and the heat conduction analogy, a review of transient SEA analysis capability was undertaken to assess the feasibility of implementing transient EFEA capability. Furthermore, a number of issues that will need to be addressed upon implementing transient EFEA have been identified and are documented here. Also, a preliminary analysis has been conducted to verify that transient heat transfer capabilities within VASTF are indeed functional and can be adapted to accommodate transient EFEA. Conclusions have been drawn concerning an approach for implementing transient EFEA, which will be the focus of the next phase of work.

In the following section, we present a review of transient SEA capabilities and issues that will have to be addressed when transient EFEA is implemented and also demonstrate the transient heat transfer capabilities available within VAST, which will be adapted for transient EFEA.

5.1 Review of Transient SEA Analysis and Presentation of Transient EFEA Requirements

In the early stages of SEA development, Manning and Lee (1968) recognized the need to model transient noise and vibration due to shock and impulsive loads. In response, they proposed a method to model these phenomena using steady state SEA power-balanced equations. Their method was implemented and subsequently verified experimentally. Their findings showed that most of the assumptions for steady-state SEA could also be extended to transient SEA. Since then, much effort has been devoted to the study of transient statistical energy analysis. Powell and Quartararo (1987) implemented transient SEA for a beam/plate system. They demonstrated that the SEA steady state equation coefficient could also be used successfully for transient SEA analysis. Good agreement was obtained between predicted and measured SEA transient decay envelopes. They also

offered suggestions concerning suitable numerical integration schemes, and time steps and scales for transient SEA. Lai and Soom (1990a, 1990b) investigated the prediction of transient vibration envelopes for coupled systems using transient SEA. The relationship between time varying energy transfer between coupled systems and time varying energies of the subsystem were developed and studied numerically and experimentally. They introduced the concept of a 'time varying coupling loss factor' to account for transient analysis. They concluded from their studies that the use of steady state (i.e., time invariant) coupling loss factors may be acceptable for overall response in many situations, and also that the coupling loss factor used to compute the total response is the same as the steady state coupling loss factor. However, they cautioned that the steady state coupling loss factor might not be suitable for use with low-frequency bands. Honda and Irie (1995) successfully studied transient vibration based on SEA using the concept of state space and transition matrices. Step, impulse, and reverberant process inputs were used in the transient study.

Pennington and Lednik (1991, 1996a, and 1996b) studied transient response of multi-degree-of-freedom system subjected to an impulse, and compared the result to transient SEA analysis of the system. They derived mathematical expressions for both methods. The comparison focused on the initial energy transfer ratio, the rise time to peak value, the peak value, and the final decay rate. They noted some interesting findings, including: (i) the integral of transmitted energy is identical for both approaches, and (ii) while the peak response is reached sooner using SEA analysis, peak levels and eventual decay rates are similar for both methods. Other studies have been conducted on transient SEA, including an investigation of methods for predicting the effective loss factor of coupled systems in quasi-transient conditions (Sun et al., 1986). Tools for transient SEA analysis have also been developed, including 'TRANSTAR' (1993).

It can be seen from the above review that methodologies for transient SEA have not only been developed and demonstrated, but have also been implemented and verified. These methods use both conventional numerical integration schemes and non-conventional state space models. Issues critical to transient SEA, such as suitable timescales and coupling loss factors, have been addressed. Results from published works on transient SEA will be used as benchmarks for the verification of transient EFEA.

A successful implementation of transient SEA is required for a meaningful implementation of transient EFEA. In light of the above noted finding, it can be said with certainty that practical implementation of transient EFEA is indeed very feasible. As noted at the beginning of this discussion, the formulation has already been presented by Nefske and Sung (1989). Some of the practical issues that will be addressed during the implementation of transient EFEA, including the definition of a suitable coupling loss factor and timescale for numerical integration, have been addressed by transient SEA. Other practical issues, such as some of the equivalent transient EFEA analogies, are similar to steady state EFEA and have been presented in Table 3-1. The only difference being that some of the variables used in the transient analogy models might have to be modeled as time varying as opposed to time invariant. A few other analogies (e.g., initial conditions and transient dynamic load representation such as shock, impulse and step

loads in the context of power flow models), which are unique to transient conditions, will have to be developed for heat transfer analogies. Furthermore, an appropriate interface will have to be developed for linking with the existing transient heat transfer capabilities of VAST (which will be adapted for the transient analysis) and interpreting transient power flow inputs such as load representation and outputs such as rise times, energy envelopes, peak velocities/energies, settling times, and transmitted energy estimates.

6. HABITABILITY and UNDERWATER RADIATED NOISE

Under the work previously performed by Martec for DRDC Atlantic (then Defence Research Establishment Atlantic), a rudimentary capability for predicting underwater radiated noise was formulated (Smith and Chernuka, 1997), but was never fully implemented into the SNAP software. In this section, a brief review of that work is discussed along with some insight into the work developed by other researchers (Termeer and Jong, 1998a), (Termeer and Jong, 1998b),

A distinction must first be made between the interior and exterior radiated noise problems. In almost all cases, interior noise analysis will involve the prediction of a reverberant acoustic field. While in some particular cases a direct acoustic field may be of importance (and this will be addressed during this project), habitability issues will almost always involve predicting the reverberant room noise. On the other hand, predicting the external underwater radiated noise will involve a semi-infinite fluid domain where the acoustic field will never be reverberant and the predicted radiated noise levels will vary with position in the acoustic field.

6.1 Interior Noise

It was shown that, for a diffuse sound field, the sound propagated to an interior space is assumed to be reverberant and the energy density, E , in the space is given by:

$$\frac{-c^2}{\omega\eta} \nabla^2 e + \eta\omega e = \pi_{in} \quad [6-1]$$

where π_{in} is the power input (per unit volume) to the system and η is the loss factor of the fluid medium (characterized by sound speed, c and density, ρ). It was also shown that this loss factor can be represented as the product $\omega\tau$ where τ is the relaxation time for the space (time for the sound field to decay by 60 dB).

Another way to represent the total dynamic energy of an acoustic space with volume V is (Termeer and Jong, 1998a):

$$e = V \frac{\langle p^2 \rangle}{\rho c} \quad [6-2]$$

where $\langle p^2 \rangle$ is the space- and time-averaged squared pressure in the acoustic space.

The active intensity component is that related to the net transport of energy and it was shown that the active intensity vector, \vec{I} , is given by:

$$\vec{I} = \frac{-c^2}{\omega\eta} \nabla e \quad [6-3]$$

and that a boundary condition based on the power absorbed at the bounding surfaces of the volume (under steady state) can be represented as

$$\vec{I} \cdot \vec{n} = \frac{1}{4} \alpha c e \quad [6-4]$$

where \vec{n} is the outward unit normal from the surface and α is the local Sabine coefficient for the surface. The Sabine coefficient is a measure of acoustic absorption of the surfaces and is described by the Sabine equation (Bies and Hansen, 1998) as:

$$\tau = \frac{55.25V}{S\bar{\alpha}} \quad [6-5]$$

where S is the surface area of the boundary and $\bar{\alpha}$ is the mean Sabine absorption coefficient. The above two intensity equations can be used as boundary conditions to solve the energy equation. This formulation was not implemented in the SNAP software and should be evaluated and compared with other techniques for evaluating interior noise fields.

It should be noted that the most difficult task may well be the establishment of appropriate absorption coefficients. Also, as mentioned above, further development will be required to establish a direct sound field where desirable.

6.2 Radiated Noise

The above discussion was centered on the prediction of the noise field in the enclosed space, but did not discuss the radiation mechanism into that space. Sound may be generated from within the space itself (such as a loudspeaker or a vibrating machine), but may also be generated from the boundaries of the space (the vibrating wall). In this section, we will discuss the mechanisms of radiated noise and its applications to both interior and exterior problems.

It should be noted that the sound will be assumed to be generated by flexural waves propagating in the panels bounding the acoustic medium. While in-plane vibrations will be computed by the PFEFEA software, they do not radiate in any significant way to the adjoining space, although, if they are converted to flexural waves at a structural junction, they must then be accounted for in the radiated noise prediction.

Of particular interest to the question of radiated noise to a space is the question of the critical frequency. Vibrational energy traveling through a structure radiates best to a surrounding fluid when the wave speed in the structure (c_p) matches the wave speed in the fluid. Vibrational energy traveling through a structure radiates best to a surrounding fluid at higher frequencies and poorly at lower frequencies where the wavelength is so long that the energy is not easily transferred out of the structure. The radiation to an acoustic space is defined based on the relationship of the frequency of the flexural wave to this critical frequency (f_c) for that particular physical situation. For our purposes, the physical situation is best modeled as a baffled panel (stiffened plate structure) and this critical frequency is defined as (Smith and Chernuka, 1997), (Termeer and de Jong, 1998a):

$$f_c = \left(\frac{c_0^2}{2\pi} \right) \left(\frac{\rho h}{B} \right)^{\frac{1}{2}} \quad [6-6]$$

where h is the plate thickness and $B (= Eh^3/12(1-\nu^2))$ is the bending stiffness of the panel (with Young's modulus, E , and Poisson's ratio, ν). For a steel plate in water, this equation reduces to (Feit, 1998):

$$f_c = 9300/h$$

for frequency measured in Hz and plate thickness measured in inches. Feit (Feit, 1998) also gives an approximation for the flexural wave speed in a steel plate as:

$$c_p = 612\sqrt{fh}$$

for frequency f and thickness, h , also measured in inches. At the critical frequency, the flexural wave speed and wavelength equal the acoustic wave speed and wavelength. For our notional naval frigate with structural water-loaded hull panels (between stiffeners) of size 0.5m by 1.0m with a thickness of 9mm, the critical frequency is roughly 26 kHz.

For many shipboard structural analyses, it is likely that the acoustic radiation of interest will fall below the critical frequency. However, as there may be significant energy at the lower frequencies, even with poor radiation efficiency, and should not be ignored.

Analytical solutions for general structural configurations are unlikely to be available and, as such, simplifications must be made in order to develop some viable solution techniques. Typically for ship structures at high frequencies, the radiation of a single panel can be treated as that of a radiating panel imbedded in a larger surface thus, a baffled plate. Unbaffled plates, particularly at lower frequencies, require special treatment due to radiation from the edges of the panel. For a baffled plate, the formulation is also different depending on whether the panel is simply vibrating indirectly (reverberant) or is directly loaded.

6.2.1 Reverberant Panel

For a panel without a source (i.e., reverberant structure), the radiated sound power to the surrounding fluid (ρc) is given by:

$$\Pi_{RAD} = \sigma(\omega) \rho c S \langle v^2 \rangle \quad [6-7]$$

where $\langle v^2 \rangle$ is the mean square velocity over the plate (typically the response predicted by the SNAP software). The key to this solution is the determination of the radiation coefficient $\sigma(\omega)$, which is frequency dependent. Smith and Chernuka (Smith and Chernuka, 1997) give an example of expressions for radiation efficiency based on work by Maidanik (Maidanik, 1962). At low frequency the odd modes radiate efficiently – which is difficult to model with an SEA approach.

For a stiffened panel, Maidanik noted that the stiffeners effectively increase the radiation efficiency, by a factor estimated as $(1 + 2L_s/L_p)$ where L_p is the panel perimeter and L_s is the total length of the stiffeners.

The radiated noise may also have a directional component which is frequency dependent. In reference [1], it is pointed out that for farfield radiation, the panel may be treated as a monopole source for low frequencies (well below critical frequency), but the pattern will change as frequency increases, first going to a dipole like source, then highly concentrated into narrow beams. These patterns will have to be assessed for any given problem.

6.2.2 Panel with Applied Load

For the same panel with a point force, F , which is termed direct radiation, the calculation becomes more complicated. The energy density ($e(r, \theta)$) can be represented as:

$$e(r, \theta) = \frac{k^4 |F|^2}{16\pi^2 \omega^2 \rho} \left[\frac{2}{r^2} |f(\theta)|^2 + \frac{1}{k^2 r^4} \left(|f(\theta)|^2 + |f'(\theta)|^2 \right) \right] \quad [6-8]$$

where k is the acoustic wavenumber, r is the distance to the measurement point in the field and $f(\theta)$ is a directivity function. Note that the second term goes to zero for the farfield case ($kr \gg 1$). The farfield intensity, \vec{I} , is given as

$$\vec{I}(r, \theta) = ce(r, \theta) \hat{r} \quad [6-9]$$

where \hat{r} is the unit direction vector to the field point. For frequencies well below the critical frequency, the total power radiated to the fluid (from a point load) can be calculated and, is shown in [1] to be:

$$\Pi_p = \frac{\rho |F|^2}{4\pi c m^2} \quad [6-10]$$

where m is the mass per unit area of the panel.

Although their use may not come up frequently in this project, a similar analysis can be performed for an applied moment or a line force (F'). The applied moment can be shown to be similar to a pair of opposed forces while, for the same panel with an applied line force, a similar derivation can show:

$$\Pi_i = \frac{\rho |F'|^2}{4\omega m^2} \quad [6-11]$$

6.2.3 Energy Fields

In general, it is necessary to calculate the energy and intensity fields radiated by the vibrating structure. The total radiated energy will be a summation of the reverberant energy and the directly radiated energy, or

$$E_{TOT} = E_{REV} + E_{DIR} \quad [6-12]$$

If every panel is assumed to be a point source and we assume the sources are uncorrelated, then the reverberant power from each panel, $d\Pi_{REV}$, is given by

$$d\Pi_{REV} = \sigma\rho\langle v^2 \rangle dS \quad [6-13]$$

so that the reverberant radiated energy is:

$$E_{REV} = \int_S \sigma\rho\langle v^2 \rangle G(r, \theta) dS \quad [6-14]$$

where $G(r, \theta)$ is the Green's function. If we look at a mean position in the field ($\bar{r}, \bar{\theta}$) and assume that $\langle v^2 \rangle$ is the resulting panel velocity from the power flow calculation, this reduces to

$$E_{REV} = \sigma\rho\langle v^2 \rangle G(\bar{r}, \bar{\theta}) \quad [6-15]$$

It seems likely that the same methodology used in the boundary element method to evaluate the effect of nearby bodies or free surfaces on the Green's function will be available for use in this situation.

The direct radiated energy can be calculated from the radiated power for a point and line force as

$$E_{DIR} = \frac{1}{c} \sum \Pi_p G_p(r, \theta) + \frac{1}{c} \sum_0^l \int \Pi_l G_p(r, \theta) dl \quad [6-16]$$

where the line source is represented as a distribution of l point sources.

Note that the energy calculation is only valid in the far field region of the acoustic space and is based on the calculated surface velocities of the panels. As such, it is assumed that the mass and damping effects of the fluid are already included in the calculation of the structural velocities and, so, there is no true coupling between the fluid and structural domains, i.e., there is no energy transfer back to the structure from the fluid. This is fundamentally different from the low frequency case.

6.3 Experimental Results

Experimental data to support this development will be required when the appropriate formulations are in place for the prediction of radiated noise using the PFEFEA method. A variety of data is available for simulated ship structures involving a simple box structure and a 3-bay simulated ship hull (Gilroy and Smith, 1998), (van den Tool, van der Knaap, and de Jong, 1998). DRDC is also currently constructing a simple open steel box (30cm x 60cm x 1.5m) which will be used to support the development of the PFEFEA software.

7. FLOW-INDUCED NOISE

Flow-induced noise arises from flow-induced vibrations. There are many classes of such vibrations including the familiar vortex-induced vibrations, galloping and flutter, and ocean wave-induced vibration of a riser. Of relevance to this project are those that potentially contribute to the radiated acoustic signature of surface ships. These are vibrations of ship structures that are exposed to external fluid flow (putting aside for the moment, on-board machinery noise). They are briefly summarized in Table 7-1 and include vortex shedding, fluctuating interaction loads, turbulent leading edge noise, turbulent boundary-layer, and seaway-related loads.

In the flow past a bluff body, vortices are periodically shed. Their frequency and strength depends on the geometry and characteristic length of the bluff body and the ambient flow. They create a strong oscillating pressure field immediately downstream of the bluff body. Familiar examples include flow past structural ship members and submarine periscopes.

An example of a fluctuating interaction load is that of an engine mount transmitting vibrations to the hull. These vibrations interact with the outside ambient flow past the hull at those points.

Turbulent leading edge noise arises from the fluctuating pressure field that is created when an object is cutting through water. Leading edges of keels and the ship bow are examples.

A turbulent boundary-layer is created downstream of a body moving through a fluid. The fluctuating pressure field from the turbulent boundary-layer will cause sound to radiate.

An example is the boundary-layer created on the plates of a ship hull as the ship moves through the water.

The motion of a ship caused by the seaway (as characterized by the Response Amplitude Operators) will increase the flow-induced vibration radiated from a ship through several different mechanisms. The inflow conditions to the propeller will be constantly changing and likely increasing the propeller cavitation. These motions and their interaction with the sea create fluctuating pressure fields around the ship above and beyond those of a ship going through the water in a straight line.

7.1 Modeling Flow-Induced Noise within EFEA

The basic form of the EFEA equations of motion govern the vibrational energy conduction throughout an elemental control volume of a plate or beam and can be expressed as in Section 3.2. This form is strongly analogous to the heat conduction equations and thus the conveniences of tools that quickly and readily solve such equation types are exploited.

The fluid dynamic evolution cannot, of course, be modeled within EFEA to the fidelity expected of a dedicated computational fluid dynamics (CFD) analysis code – to incorporate these phenomena into EFEA, one can model the phenomena as a distribution of oscillators defined *a priori*. The hydroacoustics of flow-driven and mechanically-driven bodies can be regarded as a superposition of spatial distributions of monopole, dipole, and quadrupole oscillators.

With a flow generated source system, the monopole is a fluctuating volume source where the source of sound is due to the fluctuation of the total mass of fluid, as in cavitation or flexural wave radiation of an elastic structure. This can be modeled as an unsteady mass injection, q' . The dipole is a fluctuating force source - a rigid surface acted on by a non-steady force will radiate sound. The fluctuating pressure field associated with the non-steady force in a compressible medium radiates sound (e.g., a turbulent boundary layer). This can be modeled as a spatial distribution of force divergence, ∇f . Finally, the quadrupole is a spatial distribution of Reynolds stress, $\partial^2 T_{ij} / \partial x_i \partial x_j$. The acoustic wave equation that expresses the field of these sources is:

$$\begin{aligned} \nabla^2 p(\bar{x}, t) - c_o^2 = -q(\bar{x}, t) + \nabla f(\bar{x}, t) - \frac{\partial^2 T_{ij}(\bar{x}, t)}{\partial x_i \partial x_j} \\ [7-1] \\ = \text{monopole} + \text{dipole} + \text{quadrupole} \end{aligned}$$

The solution to (1) can be readily described as a time-varying pressure distribution associated with the appropriate subsystems of the vibro-acoustic structure.

A knowledge of the characteristic frequency and correlation length (as shown in Table 7-1) helps determine the source and strength of the distributed monopoles, dipoles, and

quadrupoles to model the hydroacoustic phenomena, be it a turbulent boundary-layer or a propeller. These characteristic and correlation quantities can be determined through scale model measurements or CFD studies for a particular ship geometry.

The SNAP code in its present form can model flow-induced vibrations that can be modeled as distributed point sources. The energy and intensity terms for the flow-induced vibration noise sources of Table 7-1 can be obtained from the power spectral density obtained through a superposition of localized flow monopoles, dipoles, and quadrupoles to capture the flow-induced noise phenomena.

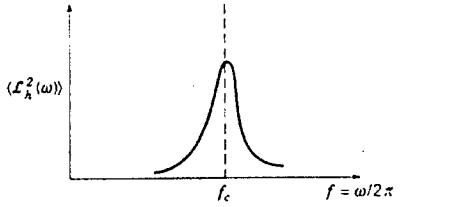
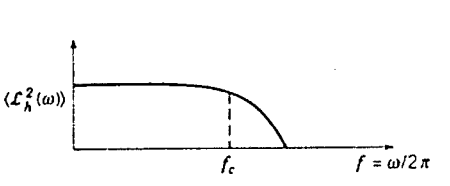
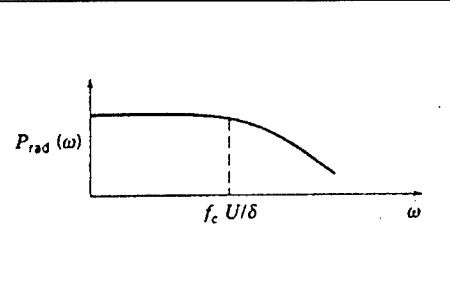
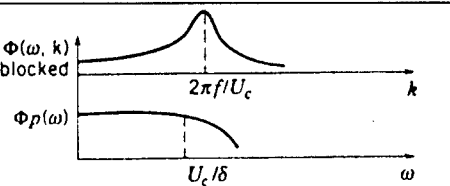
The form of the power spectral densities and, in some instances, the strength, for these sources is known and is a measure of their energy density for the excitations (Table 7-1). As such, it can be readily incorporated into the EFEA energy density and intensity equations. The location of the distributed sources is known (e.g. trailing edge of keel, leading edge of ship, hydrodynamic center of ship, propeller nearfield, etc.).

7.2 Recommendations for Implementation

The incorporation of these flow-induced noises into SNAP requires that non-stationary phenomena can be captured and processed within SNAP. This is an item slated for development in Phase II.

Phase II will focus on development and implementation for adding monopole, dipole, and quadrupole source distributions to arbitrary subsystems of a vessel. This includes adding new terms in the EFEA equations and implementation within the code. From examining the existing SNAP source code, this appears feasible.

Validation can be achieved through comparison against simple geometries in open literature or those that have analytical solutions. One example is that of sound radiated from vortex shedding off a semi-infinite plate at 90 degrees angle of attack to the flow. Another example is the fluctuating interaction load on a submerged flat plate in a flow field.

Table 7-1: Summary of flow-induced noise sources relevant to surface ships				
source type	surface ship application e.g.	characteristic frequency, f_c , and / or correlation length, l_c	frequency spectrum form	model as superposition of
vortex shedding	propeller singing, structural members, keel	$f_c d / U = 0.2$, $l_c \approx d$ ($d =$ width of body, $U =$ ambient flow)		monopole, dipole, and quadrupole
fluctuating interaction loads	engine mounts exciting engine room hull sections	$f_c = U / \lambda$ $l_c \sim \lambda$ ($U =$ ambient flow, $\lambda =$ characteristic eddy scale)		dipole
turbulent leading edge noise	bow, sonar dome, and keel	$f_c = (1/2\pi) U / \delta$ or $(1/2\pi) U / l$ $l_c \sim l$ or δ ($\delta =$ boundary-layer thickness, $P_{rad} =$ radiated sound power)		dipole, quadrupole
turbulent boundary-layer	flow over plates, frames, etc. that constitute the hull	broadband		dipole, quadrupole
seaway	ship motions and its effect on cavitation, incidence of other sources, etc.	centered around resonant frequencies for ship roll, pitch, yaw, heave, surge, sway, etc.	similar to vortex shedding	ship motion through Response Amplitude Operators and propeller radiation through monopole

8. EFEA Summary

This report presents a summary of Phase I efforts, which explored the potential of using Energy Finite Element Analysis (EFEA) methods for structural acoustic applications. A review of the development of Power Flow Finite Element Analysis (PFFEA) methodology has been presented here to assess its feasibility for use in investigating structural acoustic modeling throughout the medium- and high-frequency regimes. Also discussed are the combined efforts of Martec Limited and DRDC Atlantic over the past 10 years, during which time EFEA/PFFEA methodologies have been developed and implemented into their 'SNAP' software package. This report presents an overview of past EFEA/PFFEA research, along with a brief discussion on some of the 'SNAP' software capabilities and the theoretical foundations upon which they are based. Power flow expressions, relationships, and restrictions applicable to various structural elements, including nodes, beams, joints, and membranes, are presented. Methodologies for dealing with joints and junctions are discussed. A review of power flow strategies for fluid-loaded structures is also presented. Validation of the steady-state power flow capabilities encapsulated in the SNAP software is presented, using both Statistical Energy Analysis (SEA) and experimental results as benchmarks. Validation of the SNAP software capabilities has also been demonstrated using both simple models (e.g., beams) and more complex models (e.g., stiffened box structures). In general, results obtained via the power flow finite element approach are in good agreement with those obtained using other methods. The EFEA/PFFEA methodology, as encapsulated in the SNAP software, is shown to be an effective tool for response prediction in the medium- to high-frequency domain and can thus greatly compliment the statistical energy analysis techniques commonly used in industry today, offering the additional benefit of spatially-continuous variation of vibrational energy over the entire structure, which, in turn, allows point response predictions within a subsystem. It is hoped that existing SNAP capabilities can be enhanced such that the software can be used as a provisional tool for EFEA.

A review of transient energy techniques has also been undertaken. Findings suggest that its implementation is feasible since transient techniques have been developed and implemented for the companion methodology (SEA). Of practical interest during the implementation of transient EFEA are issues concerning the definition of coupling loss factors and numerical integration timescales, which have been addressed in some fashion by SEA. Issues concerning the use of steady-state EFEA analogies to develop equivalent transient EFEA analogies have also been presented (see Table 7-1). Analogies unique to transient analysis (e.g., initial conditions, dynamic load representation, etc.) will have to be developed from heat-transfer analogies. A suitable interface will be developed to link new capabilities with existing transient heat transfer capabilities and facilitate interpretation of transient power flow input.

A review of work previously performed by Martec Limited for DRDC Atlantic (formerly Defense Research Establishment Atlantic, DREA) has also been discussed, in which a rudimentary capability for predicting both interior noise and underwater-radiated noise was formulated [1] but never fully implemented into the SNAP software. The methodology for a radiated noise capability is explored for both reverberant-type acoustic

spaces and sources, as well as direct sound fields, including a demonstration of a prediction of radiation efficiency for a naval frigate-type structural panel. The implementation of flow-induced noise can be achieved through source distributions of monopoles, dipoles, and quadrupoles. Knowledge of the particulars of the flow phenomena from scale model tests or CFD analyses will be required to determine the source distributions. As well, the ability to capture non-stationary phenomena within SNAP will have to be developed.

Since the goal of the current project was to explore the potential of using PFFEAs capabilities for ship structural noise prediction, a number of recommendations are offered for the further enhancements to SNAP so that it can become a feasible tool for use in EFEA. Some of the most notable recommendations include:

- Enhancement and validation of thermal computational algorithms used for steady-state power flow analysis, offering potentially significant improvements in computational efficiency, especially during application to very complex systems;
- Development, implementation, and validation of transient modeling and computational algorithms and capabilities (the state-space approach and transient heat transfer analogy algorithms will be explored and selected for development);
- The provision of a seamlessly integrated modeling capability for generating the input model and data, a capability which does not exist in the current version of the software;
- Development, implementation, and validation of fluid-loading modeling and related computational algorithms;
- Development, implementation, and validation of techniques for defining boundary conditions;
- Preliminary demonstration of radiated and flow noise implementations;
- Development of algorithms to predict the identified flow-induced noise phenomena of interest to surface ship signatures including vortex shedding, fluctuating interaction loads, turbulent leading edge noise, turbulent boundary-layer noise, and motions due to the sea way;
- Developing provisions (above and beyond those required to accommodate non-stationary processes) to include distributed source terms in the EFEA energy and intensity equations for flow-induced noise contributions from the different phenomena / parts of the ship; and
- Enhancement of existing SNAP output/results formatting;

The above-mentioned tasks will require a combination of code developments, demonstrations, documentation, and validation, and will constitute the major undertaking during Phase II of the project.

9. SEA and EFEA Energy Methods for Noise Prediction and Control

Energy methods for noise and vibration analysis currently are very popular in engineering. These methods can provide simple answers on very complex questions about complex engineering systems like buildings, ships and aircrafts. Systems may contain a variety of structural components that are differentiated by materials and

geometry. A deterministic approach, which considers individual vibration modes, will not be productive when wide band noise and vibration are of interest. However, energy methods provides an alternative approach, which results in the computation of average noise and vibration levels over all frequencies of interest, and provide concise answers to wide band vibration and noise problems.

Statistical Energy Analysis (SEA) and Energy Finite Element Analysis (EFEA) are two methods to evaluate vibration/noise spreading from a source in a complex structure. The common word in these names is 'energy'. The core parameter, which these methods are able to determine, is energy density (energy per unit area or volume). Energy density is proportional to vibrational velocity squared. In both methods energy density is averaged over time and usually averaged through frequency band.

The controlling equation in both methods is a formulation of energy balance within and between subsystems, which together define a system. If, for example, the subject of interest is a ship, then a subsystem (or element) may be a part of hull structure such as bulkhead or deck section. The individual modes of vibration are not considered in the energy balance methods. In this sense both methods are statistical.

The principle difference between the two methods is the energy balance formulation for each element. For SEA it is assumed that energy density does not depend on coordinates inside an element. Physically this means that there is a diffusive field for each element. Energy balance in this case is expressed mathematically as a linear algebraic equation that equates the energy going in and out of each element. Energy density is unknown in this equation. The number of equations is equal to number of each element. The combination of all equations produces a system of the linear algebraic equations, which has one solution for each set of energy inputs.

For EFEA, energy balance is formulated for differential (elementary) parts of an element. Mathematically, it leads to a second order partial differential equation relative to energy density (the unknown in this equation) for each connected element. An analytical solution for partial differential equation is not practical. Numerical methods provide a feasible solution.

Finite Element Analysis (FEA) is a generic numerical method for differential equation solving. This is a very popular method to solve many engineering problems. Many FEA computer programs already exist. In accordance with FEA methods, a body of interest (beam, plate, liquid volume) is divided into an equivalent system of smaller bodies (finite elements) interconnected at points common to two or more elements (nodes). In the finite element method, instead of solving the problem for the entire body in one operation, one formulates the equations for each finite element and combines them to obtain a solution for the whole body. As always for numerical methods, the system of differential equations is converted to system of linear algebraic equations.

In the case of EFEA, solving the problem means determining the vibrational energy density at each node of the system. EFEA has two advantages. One is that the solution is

characterized by a smooth energy density gradient through an element, as well as between adjacent elements. This is not the case for SEA. The second advantage is the fact that the differential equation for energy density is similar to the equation for heat transfer. Only the coefficients for the equation terms differ. Heat transfer FEA algorithms and computer programs are well developed, commercially available and may be easily adopted to solve acoustical problems.

EFEA is a relatively new method and does not have a long history with ship acoustics problems whereas SEA is used in commercially available programs and has been validated for problems in the marine field.

SEA requires fewer computing resources than EFEA, if the average energy of a subsystem is the subject of interest. However, EFEA may provide a level of detail, which is not achievable for SEA. The following example illustrates this last point:

Consider a platform that has dimension 15 ft by 10 ft. For SEA, this platform would be treated as a subsystem (one element) in a system. The energy balance equation for this element is just one linear algebraic equation. For EFEA, the platform should be divided into smaller parts in order to describe the energy density gradient with sufficient accuracy. Assume each element is rectangular and has a size of 5 ft by 2 ft. This means that the system is comprised of 15 (3 by 5) elements and 24 nodes. In accordance with FEA technology the problem will be solved through the solution of 24 simultaneous linear algebraic equations. The order of the equation system for EFEA may be 20 or more times than that for an equivalent SEA system. This would seem to suggest that SEA would be preferable to EFEA. However, if the platform in this example contains an acoustic source and one needs to quantify vibration level decay from source to boundary, then SEA cannot be used and EFEA is the only viable method.

This example shows that EFEA may be very useful where a remarkable vibration level gradient is expected. Extensive experience with SEA for ship noise prediction shows satisfactory results for areas not adjacent to sources. However, in marine practice most noise and vibration analysis must include a nearby acoustic source. Existing SEA algorithms use empirical formulae to describe vibration decay from sources to boundaries. In this case the combination of SEA and EFEA methods in one package looks promising. The possible approach for this combination is described below.

Output from an EFEA program, such as SNAP, is stored in an ASCII file that includes node number and energy density at each node. This EFEA program is used in the vicinity of the acoustic source where energy density gradients may be large. For example, it may be a tank top in an Engine Room restricted by bulkheads and side structures. Energy density may be averaged along connections with adjacent elements. An averaged energy density will be used to calculate energy flowing into adjacent elements. Past the machinery room boundaries SEA algorithms will be used. Such an approach does not require significant increase in computer resources as EFEA will be used on a limited area.

10. EFEA implementation in practice.

To establish an EFEA program as a practical tool, additional research should be performed. The following issues are subjects for phase II of the current contract.

Currently, EFEA algorithms have been realized in a software package named SNAP (Structural Noise Analysis Program) developed by DRDC and Martec Ltd. To date this program has been used basically as a research tool. However, the program may be converted to a generic noise analysis program

The following issues are critical.

1. The principles for *discretization* should be developed. On one hand, the use of MAESTRO²-like models, which are used for other applications (such as the strength or vibration of an entire ship) would seem attractive. Such models are relatively detailed containing thousands of nodes. On the other hand, one should keep in mind that the program should be run many times for different frequencies. A multi-thousand order of equation system may be not practical to use in routine design procedures. The order of the system will be reduced if size of element is increased. An EFEA model will meet algorithm restrictions when the modal overlap is more than unity, which is possible with larger element sizes. Size optimization depends on expected energy density gradient. The comparison of measured and calculated results may give an opportunity to make some correction in algorithms, to change *discretization* approach and to adjust loss factors as a function of frequency. Obviously, the element size near a source is expected to be smaller than one further from the source.
2. Some elements have external energy input from a known vibration source. However, energy is not an easily measurable parameter. Conversion of measured vibration levels to energy is one of the essential problems for EFEA implementation. Some additional effort is planned to convert measured vibration levels to nodal input power.
3. Modeling the acoustic space and predicting sound pressure in the acoustic space is not currently incorporated in SNAP. Well-known radiation algorithms will be used to calculate noise levels in compartments. Structural response to airborne noise is not an issue for rooms without sources. The approach is similar to that existing in *Designer Noise*TM. There are multiple validations of this approach for actual designs. Methods for predicting farfield underwater radiated noise have been proposed and need to be incorporated in the program
4. Transient load will be incorporated into SNAP algorithms and software based on interdisciplinary data. Time dependence, coordinates for impact, load amplitude will be assumed as known. External force nodal distribution algorithms are subjects for further development. This will allow for the incorporation of a flow noise and underwater shock capability into the software.

² Commercially available FEA software from Anteon/Proteus used with the SNAP software.

5. NCE believes that different acoustical tasks, such as underwater noise, inboard noise and platform noise, should be able to use common algorithms located in a program suite together with structural modeling capability. SNAP has potential to be incorporated in such an integrated system.

The combination of EFEA, via SNAP, in machinery spaces and the existing SEA driven "Designer Noise™" software will provide a tool that allows the user to accurately map the flow of vibration near the source and then utilize simpler but accurate algorithms to attenuate the energy as it flow through adjoining compartments. This would be a significant improvement.

11. References

1. Bies, D.A., Hansen, C.H., "Sound Absorption in Enclosures," Handbook of Acoustics (M. J. Crocker, ed.), John Wiley & Sons, New York, 1998.
2. Burrell, S.C. "Dynamic Structural Response using Power Flow Finite Element Analysis, MASC Thesis, Technical University of Nova Scotia, Halifax, Nova Scotia, 1998.
3. Burrell S.C. and Chernuka, M.W. "Extension of Power Flow Finite Element Analysis to Ship Structures, Part 1, Martec Limited, Halifax Nova Scotia, 1990.
4. Burrell, S.C., Orisamololu, I.R. and M.W. Chernuka, "Extension of Power Flow Finite Element Analysis to Ship Structures, Part 2, TR-92-9, Martec Limited, Halifax Nova Scotia, 1992.
5. Burrell, S.C., Liu, Q. and Chernuka, M.W. "Extension of Power Flow Finite Element Analysis to Ship Structures, Part 3, TR-92-18, Martec Limited, Halifax Nova Scotia, 1992.
6. Feit, D., "Sound Radiation from Marine Structures," Handbook of Acoustics (M. J. Crocker, ed.), John Wiley & Sons, New York, 1998.
7. Gilroy, L.E., Smith, M.J., "High Frequency Response of a Stiffened Box Structure," DREA Technical Memorandum 98/227, 1998.
8. Honda, I. and Irie, Y. "Transient Energy Borne Analysis by Using SEA," Proceeding of Internoise, July 10-12, 1995.
9. Iadevaia, M., Hal Val, B., Riobbo, J.L., and Sas, P., "Using Statistical Energy Analysis for Shock Pulse Predictions," Proceedings of ISMA 2002, pp.2337-2342, 2002.
10. Junger, M.C. and Feit, D., Sound, Structures and Their Interaction, 2nd Ed., The MIT Press, Cambridge, MA., 1986.
11. Lai, M. L and Soom, A., Prediction of Transient Vibration Envelops Using Statistical Energy Analysis Techniques, Journal of Vibration and Acoustics, vol 112 (1),pp 127-137, 1990.
12. Lai, M. L and Soom, A., Statistical Energy Analysis for the Time Integrated Transient Response of Vibrating Systems, Journal of Vibration and Acoustics, vol 112 (2),pp 206-213, 1990.
13. Lednik, D. and Pennington, R.J., "A Study of High Frequency Vibration Due to Pyrotechnic Shocks in Coupled Systems," Proceedings of the International Conference on Spacecraft Structures and Mechanical Testing, 24-26 April, 1991, Noordwijk, The Netherlands, 1991.
14. Lee, Y.A and Tolomeo, J., "An Integrated Acoustic Analysis Capability," Proceedings of ESTECH 2001, 2001.
15. Maidanik, G., "Response of Ribbed Panels to Reverberant Acoustic Fields," The Journal of the Acoustical Society of America, Vol. 34, No. 6, pp. 809-826, 1962.
16. Manning, J.E., and Lee, K., "Predicting Mechanical Shock Transmission," Shock and Vibration Bulletin, Vol. 37, No. 4, pp. 65-70, 1968.
17. Mercer, C.A., Rees, P.L. and Fahy, F.J., "Energy Flow Between Two Weakly Coupled Oscillators Subject to Transient Excitation," Journal of Sound and Vibration, Vol. 15, No. 3, pp 373-379, 1971.

18. Nefske, D.J., and Sung, S.H., "Power Flow Finite Element Analysis of Dynamic Systems: Basic Theory and Application to Beams," *Journal of Vibration, Acoustics, Stress and Reliability in Design*, Volume 111, January, 1989.
19. Penning, R.J. and Lednik, D., "Transient Statistical Energy Analysis of an Impulsive Excited Two Oscillator System," *Journal of Sound and Vibration*, 189(2), pp.249-264, 1996.
20. Penning, R.J. and Lednik, D., "Transient Energy Flow between Coupled Beams," *Journal of Sound and Vibration*, 189(2), pp.265-287, 1996.
21. Powell, R.E and Quartararo, L.R., "Statistical Energy Analysis of Transient Vibration," ASME Winter Meeting, Boston MA, 1987, *Statistical Energy Analysis*, Book No. NCA-Vol 3, K.H. Hsu, D.J. Nefske, and Aaky Eds., pp.3-7, 1987.
22. Singh, A.K., "Shock Environment Prediction of Isolated Equipment by TRANSTAR SEA Program", *Proceedings of Institute of Environmental Science*, 1993.
23. Smith, M.J. and Chernuka, M.W., *Extension of Power Flow Finite Element Analysis to Ship Structures*, Technical Report TR-95-31, Martec Limited, Halifax Nova Scotia, 1996.
24. Smith, M.J. and Chernuka, M.W., *Validation of Power Flow Models For Plate-Beam Systems – Experimental Design*, Technical Report TR-96-04, Martec Limited, Halifax Nova Scotia, 1996.
25. Smith, M.J. and Chernuka, M.W., *Advanced Modeling Capabilities for Power Flow Finite Element Analysis (PFEEA)*, Technical Report TR-97-07, Martec Limited, Halifax Nova Scotia, 1996.
26. Smith, M.J., *A Hybrid Energy Method for Predicting High Frequency Vibrational Response of Point-Loaded Plates*, *Journal of Sound and Vibration*, 202 (3), 375-394, 1997.
27. Smith, M.J., Chernuka, M.W., "Advanced Modeling Capabilities for Power Flow Finite Element Analysis," *DREA Contractor Report CR/97/447*, 1997.
28. Smith, M.J. and Brennan, D.P., *Verification and Extended Application of Power Flow Finite Element Analysis (PFEEA) for Ship Structures*, Technical Report TR-98-20, Martec Limited, Halifax Nova Scotia, 1998.
29. Sun, H.B., Sun, J.C. and Richards, E.J., "Prediction of Total Loss Factors of Structures Part III: Effective Loss Factors in Quasi-Transient Conditions," *Journal of Sound and Vibration*, Vol. 106, No. 3, pp. 465-479, 1986.
30. Termeer, M.K., de Jong, C.A.F., "Statistical Energy Analysis Applied to Ship-like Structures, Part I: Air-borne Noise Radiation," *TNO report HAG-RPT-980080*, 1998.
31. Termeer, M.K., de Jong, C.A.F., "Statistical Energy Analysis Applied to Ship-like Structures, Part I: Underwater Noise Radiation" *TNO report HAG-RPT-980171*, 1998.
32. van den Dool, T.C., van der Knaap, F.G.P., de Jong, C.A.F., "NAH Experiments on a Triple Section Ship-like Structure" *TNO report HAG-RPT-980063*, 1998.
33. *Vibration and Strength Analysis Program (VAST) User's Manual*, Version 6.1, Martec Limited, Halifax, Nova Scotia, Canada, 1996.
34. *Vibration and Strength (Field) Analysis Program (VASTF) User's Manual*, Version 6.1, Martec Limited, Halifax, Nova Scotia, Canada, 1996.